THESIS

THE INFLUENCE OF LATERAL HYDROLOGIC CONNECTIVITY ON FLUVIAL FLUX AND ECOSYSTEM METABOLISM IN A RIVER-FLOODPLAIN SYSTEM

Submitted by

Pamela Wegener

Department of Ecosystem Science and Sustainability

In partial fulfillment of the requirements

For the Degree of Master of Science

Colorado State University

Fort Collins, Colorado

Summer 2016

Master's Committee:

Advisor: Tim Covino

Stephanie Kampf
Ellen Wohl

ABSTRACT

THE INFLUENCE OF LATERAL HYDROLOGIC CONNECTIVITY ON FLUVIAL NUTRIENT FLUX AND ECOSYSTEM METABOLISM IN A RIVER-FLOODPLAIN SYSTEM

Within mountainous watersheds and river networks, low-gradient valley bottoms can function as locations of high retention and biogeochemical processing. We evaluated hydrologic dynamics, nutrient flux, and aquatic ecosystem metabolism across the snowmelt hydrograph from May – October 2015 along two river segments of the North Saint Vrain Creek, Rocky Mountain National Park, Colorado: a valley-confined channel (confined segment) and an unconfined wet valley (unconfined segment) directly downstream. We observed significant differences in water, carbon, and nutrient flux, ecosystem metabolism, and lateral hydrologic connectivity dynamics among these contrasting segments. The confined segment was a consistent source of water, carbon, and nutrients and exported 14.4 mm of water, 26 g NO_3-N ha^{-1}, 41 g dissolved organic nitrogen (DON) ha^{-1}, and 721 g dissolved organic carbon (DOC) ha^{-1} per 100 m of river length over the study period. In contrast, the unconfined segment exhibited variable source-sink dynamics and stored 1.2 g NO_3-N ha^{-1} and 1.8 g DON ha^{-1}, and exported only 1.1 mm of water and 8 g DOC ha^{-1} per 100 m. The retention of water, DOC and N related to the strength of lateral connectivity between the river and the floodplain, which in turn, influenced fluvial ecosystem metabolism rates. Gross primary productivity (GPP) and ecosystem respiration (ER) rates were higher and more variable in the unconfined versus confined river segment; average GPP was +1.01 ± 0.76 g O_2 m^{-2} d^{-1} and ER was -1.77 ± 1.10 g O_2 m^{-2} d^{-1} in the

unconfined segment, whereas average GPP was +0.09 ± 0.14 g O_2 m^{-2} d^{-1} and ER was -0.72 ± 0.50 g O_2 m^{-2} d^{-1} in the confined segment. We found that along the unconfined segment, metabolism rates generally increased from high to low flows and that the greatest increases occurred in a floodplain side-channel with intermittent surface water connections with the main channel. Combined, our data suggest a conceptual model where DOC and N are delivered to floodplain water-bodies via lateral hydrologic connections during high flows, and are subsequently utilized when velocities decline and processing rates are maximized.

TABLE OF CONTENTS

ABSTRACT ii
1. INTRODUCTION 1
2. METHODS 5
2.1. STUDY SITE 5
2.2. STREAM DISCHARGE, HYDROLOGIC FLUXES, AND CONNECTIVITY 7
2.3. DISSOLVED NUTRIENT CONCENTRATIONS AND FLUXES 9
2.4. ESTIMATING METABOLISM FROM DIURNAL DISSOLVED OXYGEN CURVES 10
3. RESULTS 14
3.1. STREAM DISCHARGE, HYDROLOGIC FLUXES, AND CONNECTIVITY 14
3.2. DISSOLVED NUTRIENT CONCENTRATIONS AND FLUXES 17
3.3. DISSOLVED OXYGEN AND FLUVIAL ECOSYSTEM METABOLISM 19
4. DISCUSSION 23
4.1. HOW DO WATER, NITROGEN, AND CARBON FLUXES VARY BETWEEN A CONFINED AND UNCONFINED RIVER SEGMENT WITHIN THE SAME NETWORK? 23
4.2. HOW DOES ECOSYSTEM METABOLISM AND ASSOCIATED NUTRIENT PROCESSING VARY AS A FUNCTION OF LATERAL CONNECTIVITY? 27
4.2.1. CONTRASTING ECOSYSTEM METABOLISM DYNAMICS ALONG A CONFINED AND UNCONFINED SEGMENT AS A FUNCTION OF LATERAL CONNECTIVITY 28
4.2.2. CONTRASTING ECOSYSTEM METABOLISM DYNAMICS IN FLOODPLAIN SURFACE WATER-BODIES AS A FUNCTION OF LATERAL CONNECTIVITY 31
5. CONCLUSIONS 35
6. FIGURES 37
7. TABLES 49
8. REFERENCES 53
9. APPENDIX A 58

INTRODUCTION

Relative to their spatial extent, low-gradient, unconfined river-floodplain systems can disproportionately influence hydrologic, nutrient, and organic matter retention and processing dynamics in river networks (Lamberti et al. 1989, Pinay et al. 1994, Bayley 1995, Cirmo and McDonnell 1997). During high flows, unconfined river-floodplain systems can reduce stream power by redistributing water laterally across the floodplain, whereas more confined river segments respond to increased flow primarily by increasing stream velocity and depth (Montgomery and Buffington 1997). Water that is laterally redistributed along unconfined rivers during high flows can become temporarily stored in floodplain surface water-bodies such as side-channels and ponds (Junk et al. 1989), and can subsequently infiltrate into the subsurface and be released during low flow conditions (Mertes 1997). As such, river floodplain exchanges along unconfined river segments can serve to attenuate peak flows and maintain high water tables during low flows, with important implications for drought and flood mitigation practices (Hey et al. 2012).

Along unconfined river-floodplain systems, lateral hydrologic exchanges can facilitate the movement of nutrients (e.g., N, P) and organic matter between the river and the floodplain via surface (Junk et al. 1989) and subsurface (Tockner et al. 2000) flowpaths. During overbank flood pulses, nutrients and suspended sediment can be delivered from the river and deposited on the floodplain (Mitsch et al. 1979), while labile organic matter can be transported from the floodplain to the river network (Junk et al. 1989, Ward and Stanford 1995, Tockner et al. 1999). In addition to overbank flood pulses, subsurface connections can also facilitate dissolved organic carbon (DOC), nitrogen (DON), and nutrient exchange between the river and floodplain

(Tockner et al. 1999, Tockner et al. 2000). Surface and subsurface lateral connections across the river-floodplain can establish linkages between nutrient sinks and sources, which can stimulate biogeochemical processing along the river network (Junk et al. 1989, Tockner et al. 2000, Powers et al. 2012).

Subsequent to delivery of organic material and nutrients during high flows, hydrologic residence times within floodplain surface water-bodies can influence nutrient and organic matter processing and downstream export patterns (Powers et al. 2012). At lower flow states, floodplain surface water-bodies can become disconnected from the main channel, and can switch from operating under lotic (i.e., advective) to lentic (i.e., standing water) conditions. As surface water-bodies disconnect from the main channel and become increasingly lentic, elongated residence times can extend the duration of direct contact between microbes and substrate, which can facilitate high rates of nutrient and organic matter processing (Battin et al. 2008). As such, rates of nutrient and organic matter processing in floodplain surface water-bodies should presumably increase as the water-bodies become disconnected from the main channel. However, data to support these assumptions are scarce, as estimates of ecosystem processing tend to be qualitatively inferred from nutrient and organic matter concentrations and fluxes (e.g., Tockner et al. 1999), rather than quantified directly using gas change methods (Odum 1956, Bott 1996) or [^{14}C] bicarbonate additions (Vollenweider 1974, Bott 1996).

In addition to within floodplain water-bodies, direct measurements of ecosystem processing rates as a function of lateral connectivity are also scarce within the main channel. In mountainous watersheds, rivers often alternate between confined valleys (low lateral connectivity) and unconfined valleys (dynamic lateral connectivity) (Stanford and Ward 1993) with implications for downstream export patterns. While these alterations seemingly provide an

excellent opportunity to investigate the effects of lateral connectivity on ecosystem processing, few studies address linkages between geomorphology and ecosystem processing on the river segment scale. One exception, Bellmore and Baxter 2014, found that an unconfined river segment in central Idaho had higher rates of primary productivity and similar rates of ecosystem respiration relative to a confined segment of the same river (Bellmore and Baxter 2014). However, these conclusions were based on a single data point during the summer baseflow period (Bellmore and Baxter 2014), and therefore do not address the responses of each river segment to temporal variability in lateral hydrologic connectivity.

The growing availability of automated data-logging dissolved oxygen (DO) probes has made continuous aquatic ecosystem metabolism data increasingly attainable by way of the diurnal DO change method (Tank et al. 2010). Aquatic ecosystem metabolism metrics gross primary productivity (GPP) and ecosystem respiration (ER) are integrative measures of the processes controlling nutrient and organic matter cycling, and can serve as functional indicators of stream health (Young et al. 2008). GPP is the rate at which inorganic carbon (CO_2) is converted to organic carbon by autotrophs (e.g., benthic algae, macrophytes, and phytoplankton) during photosynthesis, and ER is the rate at which organic carbon is converted to CO_2 by autotrophs and heterotrophs (e.g., microorganisms, meiofauna, and macrofauna) during respiration. The balance between GPP and ER (net ecosystem productivity; NEP) indicates whether an ecosystem is net autotrophic (positive NEP) or net heterotrophic (negative NEP).

In dynamic river-floodplain systems, the strength and type of lateral hydrologic exchanges influences spatiotemporal patterns in fluvial ecosystem metabolism, yet remains a poorly understood topic in watershed science. Because low-gradient, unconfined river-floodplain segments can be key locations in the river network for hydrologic and biogeochemical retention

and processing, (Lamberti et al. 1989, Bayley 1995, Cirmo and McDonnell 1997), it is important to better understand the relationships between lateral connectivity, flux, and ecosystem metabolism in these environments. This is particularly true as constructed riparian wetlands are commonly built using compacted clay substrate and periphery berms, which limit river-floodplain connectivity (Whittecar and Daniels 1999) and reduce the opportunities for these wetlands to provide flood protection and improve downstream water quality (Hey et al. 2012). Natural riparian wetlands, in contrast, can have highly dynamic river-floodplain interactions as a function of discharge, with considerable bidirectional movement of water and associated material across flow states. The goal of this research was to determine the relationships between (1) lateral hydrologic connectivity, (2) water, nutrient, and carbon fluxes, and (3) ecosystem metabolism in a confined- and an adjacent (directly downstream) unconfined- river segment of North Saint Vrain Creek in Rocky Mountain National Park, Colorado (Figure 1). To address this overarching goal, we ask the following questions:

1) *How do water, nitrogen, and carbon fluxes vary between a confined and unconfined river segment within the same network*?
2) *How does ecosystem metabolism and associated nutrient processing vary as a function of hydrologic connectivity?*

2. METHODS

2.1 Study site

This research occurred in the 88 km^2 Wild Basin Watershed, located in the southeast corner of Rocky Mountain National Park, CO (40°13'N, 105°32'W) (Figure 1). North Saint Vrain Creek, which drains Wild Basin, flows east from the Continental Divide at 4046 m to 1945 m at the base of the Rockies. We conducted fieldwork May – October 2015 on two river segments in North Saint Vrain Creek: 1) a confined single-thread reach (hereafter referred to as "confined segment"), and 2) an unconfined multi-thread network with side channels, ponds, and riparian wetlands (hereafter referred to as "unconfined segment") formed from multiple beaver dams and located directly downstream from the confined reach (Figure 1). The confined and unconfined segments are located above a Pleistocene terminal moraine and overlie Precambrian-age Silver Plume Granite (Braddock and Cole 1990). Wild Basin contains variable stand ages, including a number of old-growth stands in which trees germinated prior to 1654 A.D. (Sibold et al. 2006). Upland vegetation consists of engelmann spruce (*Picea engelmannii*), subalpine fir (*Abies lasiocarpa*), and lodgepole pine (*Pinus contorta*), and valley bottom vegetation consists of quaking aspen (*Populus tremuloides*), dense stands of willow (*Salix* spp.) and other riparian shrubs. Mean annual temperature is 5°C, with a winter average of -4°C and summer average of 14°C for the 27 years of recorded temperature data (1988-2015) (Copeland Lake snowpack telemetry, SNOTEL, #412, 2620 m elevation located within Wild Basin). Mean annual and mean summer temperature were typical in 2015 relative to historic values (6°C and 15°C, respectively), while the mean winter temperature was warmer than historic values at -1°C. Annual precipitation averaged 861 mm for 30 years (1985-2015), with 52% (451 mm) in the

form of snowfall. There was slightly less precipitation in 2015 than average (813 mm), although the distribution of precipitation was skewed toward winter precipitation with 64% (519 mm) in the form of snowfall (SNOTEL, #412). There is a strong elevation gradient in precipitation and snow totals in the watershed, with intermittent snow typical at the Copeland Lake SNOTEL site and a persistent snowpack typical at higher elevations in the watershed, extending from October 29th to June 5th in 2015 (Wild Basin SNOTEL, #1042, 2914 m). The North Saint Vrain Creek hydrograph is dominated by seasonal snowmelt, with peak annual discharge typically in June and baseflow typically from August – April.

The confined segment is a single-thread channel with pool-riffle morphology (Montgomery and Buffington 1997) and several channel-spanning log jams (Table 1). While a small decrease in stream width occurred from peak snowmelt in June to baseflow in August, the confined segment has limited overbank flooding and develops minimal floodplain surface water-bodies during high flows.

The unconfined segment has a multi-thread channel network, with a highly sinuous main channel that exhibits pool-riffle morphology (Table 1). Along the unconfined segment, numerous channel-spanning beaver dams have promoted enhanced vertical- (Briggs et al. 2012) and lateral hydrologic connectivity (Westbrook et al. 2006). Extensive lateral exchange of water and associated material between the main channel and the floodplain has resulted in a physically and chemically heterogeneous floodplain (i.e.,"riverscape" *sensu* (Malard et al. 2000, Tockner et al. 2000)) that consists of lotic (connected channels), semi-lotic (dead arms), and lentic (ponds) water-bodies. Lateral hydrologic connectivity facilitates nutrient and organic matter exchange between the main channel and floodplain water-bodies, and occurs via surface flow (e.g., the flood pulse concept (Junk et al. 1989)) and subsurface pathways (Ward and Stanford 1995).

We define two classifications of monitoring sites: 1) main channel monitoring sites, and 2) floodplain water-body sites. We present data from three main channel monitoring sites, which we call main channel 1 (MC1), main channel 2 (MC2), and main channel 3 (MC3). The confined segment is bracketed by MC1 and MC2, and the unconfined segment is bracketed by MC2 and MC3 (Figure 1, Table 2). At main channel monitoring sites, we monitored stage, water temperature, dissolved oxygen, and colored dissolved organic matter (cDOM) at 15-minute intervals, and took grab samples approximately once every other week to analyze for nutrients and major cations and anions. We present data from two floodplain water-body sites in the unconfined segment: a side-channel (SC1) and a pond (P1) (Figure 1, Table 2). At SC1 and P1, we continuously monitored stage, water temperature and dissolved oxygen, and took grab samples approximately once every other week to analyze for nutrients and major anions and cations. We continuously monitored stage at five additional side-channels and five additional ponds in the unconfined segment floodplain to characterize river-floodplain (lateral) hydrologic connectivity from high to low flows (Figure 1). The floodplain sites were selected in March 2015 and chosen to encapsulate a range of hydrologic connectivity to the main channel: e.g., intermittently- and never- connected to the main channel with surface water (Table 3).

2.2. Stream discharge, hydrologic fluxes, and connectivity

We recorded stage and water temperature at MC1, MC2, and MC3 at 15-minute intervals using real-time data logging capacitance rods (TruTrack WT-HR data logger, Christchurch, NZ). We developed a rating curve between stage and discharge (Q) measurements across the range of flows and used this relationship to derive continuous Q time series from real-time stage data. We measured Q at each site on a weekly basis from high to low flows using velocity-area (Dingman 2002) or dilution gauging (Kilpatrick and Cobb 1985) approaches. During dilution gauging, we

dissolved sodium chloride (NaCl) in streamwater and injected the solution instantaneously at a sufficient mixing length (50-75 m) upstream of the measurement site. We measured streamwater specific conductivity (SC) using CS547A conductivity and temperature probes (Campbell Scientific Inc. CS547A, Logan, UT) connected to CR1000 data loggers (Campbell Scientific Inc. CR1000), recording at 2-second intervals prior to the injection of NaCl to determine background concentrations, through the arrival of NaCl (i.e., the breakthrough curve), and after the stream returned to background NaCl concentrations. We converted SC to NaCl concentrations using an empirical calibration, which was then used to calculate Q from the breakthrough curve by equation 1:

Eq. 1) $$Q = \frac{NaCl_{MA}}{\int_0^t NaCl_C(t)dt}$$

where $NaCl_{MA}$ is the mass of NaCl added to the stream and $NaCl_C$ is the background corrected NaCl concentration. We converted 15-minute Q to area-normalized runoff and calculated daily and cumulative water fluxes and water balances for the confined and unconfined river segments. The confined segment balance was calculated as the difference between normalized daily runoff measured at MC2 and MC1 (Figure 1), and the unconfined segment balance was calculated as the difference between normalized daily runoff measured at MC3 and MC2 (Figure 1).

We recorded 15-minute surface water temperature and stage using capacitance rods at floodplain surface water-bodies (six side-channels and six ponds; Figure 1) with varying degrees of surface and/or subsurface hydrologic connectivity to the main channel (Table 3). We distinguished between sites with surface- and sites without surface water exchanges with the main channel based on a visual assessment of whether the site contained flowing water over the monitoring period. For all sites, we calculated mean daily elevation of the water surface based on capacitance rod data and elevation surveys using TOPCON RTK-GPS with cm accuracy

(Trimble Navigation Ltd., Sunnyvale, CA) and used abrupt changes in water levels and temperature to distinguish between high and low connectivity periods (e.g., Cabezas et al. 2011). For surface connected sites, high lateral connectivity referred to the period of time in which the sites were hydrologically inundated by overbank flooding from the main channel. For sites with no surface water connections with the main channel, shifts in the strength of lateral connectivity likely reflected transitions in subsurface flow-paths.

2.3 Dissolved nutrient concentrations and fluxes

We collected grab samples approximately once every other week at the three main channel sites, MC1 (n=11), MC2 (n=10), and MC3 (n=9), and floodplain water-body sites SC1 (n=8), and P1 (n=9) to analyze for nutrients and major cations and anions. Water samples were field filtered through 0.7μm glass fiber filters (GF/F Whatman International, Ltd., Maidstone, UK) into acid-washed and stream-rinsed 125 mL high-density polyethylene bottles, placed in a dark cooler, and frozen until analysis. Phosphate (PO_4^{3-}) and nitrate (NO_3^-) concentrations were analyzed using a Dionex ICS-3000 Ion Chromatograph, ammonium (NH_4^+) concentrations were analyzed using a Waters 580 Ion Chromatograph, and total organic carbon and nitrogen concentrations were analyzed using a Shimadzu TOC-V Combustion Analyzer at the Rocky Mountain Research Station, Fort Collins, Colorado (Pierson et al. 2016).

We monitored colored dissolved organic matter (cDOM) at 15-minute intervals using an *in situ* optical cDOM fluorometer (Turner Designs Inc. Cyclops-7, San Jose, CA) shielded against light and wired to a CR1000 data logger. CDOM refers to the portion of dissolved organic matter that contains chromophores that absorb UV and visible light and fluoresce after light absorption. Each cDOM fluorometer was calibrated using Quinine Sulfate solution ($r^2 >$ 0.99) prior to deployment. Hydro-Wipers (Zebra-Tech Turner Designs Inc. Cyclops-7) were

installed with cDOM fluorometers and programmed to wipe the sensor optics every hour to clear the surface from accumulated debris. We developed an empirical relationship between cDOM and simultaneous dissolved organic carbon (DOC) concentrations from main channel grab samples, and used that relationship to transform continuous cDOM measurements to a continuous DOC time series at main channel sites MC1, MC3, and MC3.

To calculate daily NO_3^-N, DON, and DOC fluxes along the main channel, we multiplied solute concentrations by the normalized daily mean runoff at each main channel site. We used DON and NO_3-N concentrations from grab sample data and daily mean DOC concentrations from the 15-minute time series data. The confined segment balances were calculated as the difference between solute fluxes derived at MC2 and MC1 (Figure 1), and the unconfined segment balances were calculated as the difference between solute fluxes derived at MC3 and MC2 (Figure 1).

2.4. Estimating metabolism from diurnal dissolved oxygen curves

We calculated daily gross primary production (GPP; g O_2 m^{-2} d^{-1}) and daily ecosystem respiration (ER; g O_2 m^{-2} d^{-1}) at main channel sites MC2 (confined outflow) and MC3 (unconfined outflow), and floodplain sites SC1 and P1 using the open-channel, single-station diurnal dissolved oxygen (DO) change method (Odum 1956, Bott 1996). At MC2 and MC3, we measured DO concentrations and water temperatures at 15-minute intervals from May 1st – September 28th using Ponsel optical dissolved DO sensors (Fondriest Environmental Inc. Ponsel Digisens, Fairborn, OH) and CS547A temperature probes connected to CR1000 data loggers. At SC1 and P1, we measured DO concentrations and water temperature at 15-minute intervals from June 9th – September 28th using MiniDOT optical dissolved O_2 sensors (Precision Measurement

Engineering Inc., MiniDOT, Vista, CA). Using the hourly rate of change in DO concentrations, we calculated GPP and ER with equation 2:

Eq. 2) $$\Delta DO = GPP - ER + E$$

where *E* represents the net exchange of oxygen with the atmosphere between consecutive measurements. We calculated the exchange of oxygen with the atmosphere by multiplying the average DO saturation deficit or excess with the reaeration rates determined for each study reach for each time step. Reaeration rates are predominantly a function of stream velocity in lotic sites and a function of wind velocity in lentic sites. For lotic sites MC2, MC3, and SC1, we calculated hourly reaeration rates according to the surface renewal model (Owens 1974) which first calculates a mass transfer coefficient (*f*) using equation 3:

Eq. 3) $$f_{(20°C)} = 50.8 * V^{0.67} * H^{-0.85}$$

where $f_{(20°C)}$ represents the mass transfer coefficient at 20°C (cm/h), *V* the velocity of stream flow (cm/s) and *H* the mean depth (cm). We used capacitance rod stage data to obtain *H,* and developed rating curves between *H*, width (*w*), and *Q* using the velocity-area method (Dingman 2002) to transform *H* to *V* (*Q*/*w*) data to calculate hourly $f_{(20°C)}$. We adjusted $f_{(20°C)}$ to the streamwater temperature at each sampling time following equation 4 (Elmore and West 1961):

Eq. 4) $$f_{(t°C)} = f_{20°C} * 1.024^{(t-20)}$$

where *t* represents water temperature (°C), and divided by *H* to generate reaeration coefficients (*k*, h^{-1}) at each time step. In order to determine the sensitivity of the calculated metabolism metrics to the reaeration coefficient at sites MC2, MC3, and SC1, we calculated coefficients for four different scenarios, which consisted of: 1) mean daily water velocity inputs to mass transfer coefficients at standard temperature, 2) mean daily water velocity inputs to mass transfer coefficients corrected for temperature, 3) an average water velocity input to mass transfer

coefficients at standard temperature, and 4) an average water velocity input to mass transfer coefficients corrected for water temperature (Supplemental Table 1). For lentic sites (e.g., P1), reaeration is predominantly a function of wind. We used empirically-derived equation 5 (Boyd and Teichert-Coddington 1992)

Eq. 5) $$k_{(20°C)} = 0.017X - 0.014$$

where k is the reaeration coefficient at standard temperature (h^{-1}) and X is wind speed at 3 m height (m s^{-1}) to calculate reaeration coefficients at P1 for a low wind (0.8 m s^{-1}) and high wind (4.5 m s^{-1}) scenario. The low wind velocity was determined as an average calculated coefficient for a sheltered and stagnant agricultural pond (Boyd and Teichert-Coddington 1992), and the high wind scenario was chosen as the highest wind velocity value for which equation 7 can be reliably applied, 4.5 m s^{-1} (Boyd and Teichert-Coddington 1992). To determine the sensitivity of metabolism metrics calculated at P1 to the reaeration coefficient, we calculated reaeration coefficients for five scenarios which consisted of: 1) no wind, 2) a low wind input to reaeration at standard temperature, 3) a low wind input to reaeration corrected for temperature, 4) a high wind input to reaeration at standard temperature, 5) a high wind input to reaeration corrected for temperature (Supplemental Table 1).

We corrected the hourly rate of DO change by the net exchange of oxygen with the atmosphere at each site under the different reaeration scenarios (Supplemental Table 1). To calculate ER, we averaged the corrected hourly rates of DO change from post-sunset to pre-dawn, and multiplied the average by 24 hours in the day (Figure 2). During darkness, GPP is equal to 0 and any change in the rate of reaeration-corrected DO must therefore be attributed to ER. We calculated daily GPP by integrating the difference between the hourly rate of DO change and the average hourly nighttime rate of DO change over the photoperiod (Figure 2). Daily net

ecosystem production (NEP) was calculated as the difference between daily GPP and the absolute value of daily ER.

Fluvial ecosystem metabolism metrics calculated at MC2 and MC3 likely reflect the combined influences of the main channel and hydrologically connected floodplain water-bodies to metabolism rates at the outflow of the confined and unconfined segments, respectively. However, we note that DO concentrations at MC2 and MC3 are influenced by fluvial ecosystems that may exceed the upstream boundaries of the segments delineated in our study. We calculated the DO footprint at each site using the formula $3*V/k$ (Chapra and Di Toro 1991), and determined the footprint to be 5.11 km at MC2 and 5.14 km at MC3. While stream ecosystem metabolism rates at MC2 and MC3 may therefore not reflect the influence of processing rates exclusively from the confined and unconfined segments as delineated in our study, we argue that our method is sufficient to qualitatively compare patterns in metabolism from high to low flows between valley confinement types.

3. RESULTS

3.1 Stream discharge, hydrologic fluxes, and connectivity

Water temperature in the main channel increased slightly with downstream distance, with an average of 7.4 ± 3.4°C at MC1, 7.7 ± 3.4°C at MC2, and 8.4 ± 3.6°C at MC3 over the monitoring period (Table 2). Combined for all three main channel sites, the minimum recorded water temperature was 0.5°C on May 10th and the maximum recorded water temperature was 7.2°C on August 15th. Water temperature tended to be warmer and more variable in the floodplain water-bodies than the main channel, and averaged 9.8 ± 5.9°C at SC1 and 10.4 ± 3.7°C at P1 over the monitoring period (Table 2).

Main channel runoff was predominantly driven by seasonal snowmelt, with hydrographs at the three sites rising abruptly following snowmelt in late May, peaking to values between 4.5 mm d^{-1} (MC1) and 7.0 mm d^{-1} (MC2) from June 4th – 22nd, and receding to baseflow values between 0.4 mm d^{-1} (MC2) and 1.5 mm d^{-1} (MC3) by the second week in August (Figure 3). While main channel runoff was predominantly driven by snowmelt, short-term (<1 week) increases in runoff occurred during summer rainfall events (Figure 3). Rainfall occurred during approximately 20% of the days during the monitoring period, with the majority (75%) of rainfall associated with relatively small events (<5 mm d^{-1}) that had a negligible influence on daily runoff. Daily runoff notably increased (i.e., by more than 0.5 mm d^{-1}) as a response to two storm events during the monitoring period, the June 17th and July 7th – 9th storm events, in which ~20 mm d^{-1} of rainfall were recorded at the SNOTEL station (Figure 3). From May – October, runoff averaged 2.1 ± 1.5 mm d^{-1} at MC1, 2.2 ± 1.8 mm d^{-1} at MC2, and 2.4 ± 1.3 mm d^{-1} at MC3 from

(Table 2). MC2 had the highest runoff of all sites during peak flows, while MC3 had the highest runoff of all sites during baseflow (Figure 3).

Daily and cumulative hydrologic fluxes and water balances along the confined and unconfined river segments highlight substantial differences in retention capacities (Figure 4). While the confined segment was a consistent source of water, the unconfined segment displayed variable source-sink behavior, and was a net source of water during low flows and a sink during higher flows (Figure 4A). For every 100 m of river length, the confined segment exported a total of 14.4 mm of water, whereas the unconfined segment exported only 1.1 mm of water from May – October (Figure 4B). Notably, the confined segment transported on average over 10 times more water than the unconfined segment when normalized for river length (Figure 4).

Water levels in the six side-channels and six ponds along the unconfined segment floodplain were closely related to main channel runoff (Figures 3, 5). Of the six side-channel sites, five (SC1-SC5) were intermittently connected to the main channel by overbank flood pulses (Table 3, Figure 5). The remaining side-channel (SC6) and all six ponds (P1-P6) had no surface water connections with the main channel (Table 3, Figure 5). With the exception of a small pond (P6) on the northern periphery of the unconfined segment, all floodplain water-bodies contained either flowing or standing water by the onset of monitoring on May 1st, and two side-channels and two ponds became dry by the end of monitoring on September 28th (Table 3). The pond with the active beaver lodge (P1) had the most consistent water levels of any of the side-channels or ponds, with a standard deviation of ±0.03 m compared to an average standard deviation of ±0.13 m in other floodplain water-bodies (Table 3, Figure 5).

Using abrupt inflections in floodplain water levels as a proxy for increased lateral connectivity (e.g., Cabezas et al. 2011), we found that the majority of floodplain sites

transitioned to a higher connectivity phase from May 26th – June 1st (Table 3, Figure 5). For intermittently surface water connected sites, this higher connectivity phase was associated with a shift from lentic (i.e., standing water) to lotic (i.e., advective) conditions. For sites that did not exhibit surface connectivity, higher connectivity may have reflected a shift in subsurface flow paths; for example, a transition from hydrologic connectivity to an alluvial aquifer to direct seepage inflow from the river. For intermittently surface water connected sites, we used the water level of the main channel at the start of each high connectivity phase as a threshold for surface water connection and disconnection (Reckendorfer et al. 2006, Cabezas et al. 2011). Accordingly, we found that these sites lost surface exchanges with the main channel around July 12th – 14th, consistent with field observations. While surface water connection and disconnection is generally easy to recognize in the field based on the presence or absence of flow, shifts in the strength of subsurface connectivity (e.g., transitions in subsurface flow paths) are more subtle. Water temperature dynamics have previously been used to infer subsurface flow paths and qualitatively describe the strength of subsurface river-floodplain connectivity (Arscott et al. 2001, Malard et al. 2001). For example, a sudden change in daily average water temperatures can be triggered by seepage inflow from the river, and the temperatures can then be reverted back to initial conditions after the connection subsides (Cabezas et al. 2011). With this description as a guide, we identified high subsurface connectivity periods for five out of the seven never surface connected sites using qualitative characterizations of mean daily water temperatures (Table 3, Figure 5). For these sites, the onset of the high connectivity period occurred from May 30th – June 1st, and the ending of the high connectivity period occurred from June 26th – July 12th. While we define clear "start" and "end" dates, we acknowledge that in reality, the transition from high to low subsurface connectivity was likely gradual (Tockner et al. 2000).

3.2 Dissolved nutrient concentrations and fluxes

Phosphate (PO_4^{3-}) concentrations measured from grab samples were all below the method detection level, 0.01 mg L^{-1} (Pierson et al. 2016). Main channel ammonium-N (NH_4-N) concentrations were consistently low at all locations except P1, with averages of 0.02 ± 0.01 mg L^{-1} at MC1, 0.02 ± 0.01 mg L^{-1} at MC2, 0.02 ± 0.08 mg L^{-1} at MC3, and 0.03 ± 0.02 mg L^{-1} at SC1, compared to 0.06 ± 0.08 mg L^{-1} at P1 (Table 4, Figure 6A). As the hydrograph receded, NH_4-N concentrations at P1 increased to the highest observed value by late September, 0.20 mg L^{-1}, which was approximately four times the next highest NH_4-N concentration that day, 0.05 mg L^{-1}, in MC1 (Figure 6A).

At all locations, nitrate-N (NO_3-N) concentrations trended with main channel runoff, with the highest concentrations during peak snowmelt in June (Figure 6B). NO_3-N concentrations in SC1 had the greatest range of all of the sites, with a peak value of 0.14 mg L^{-1} in early June and lows of <0.005 mg L^{-1} from August – October (Figure 6B). In contrast, NO_3-N concentrations in P1 were the most stable of all sites, with a maximum value of 0.05 mg L^{-1} in early June and lows of ~0.02 mg L^{-1} in August (Figure 6B). From May–October, NO_3-N concentrations averaged 0.07 ± mg L^{-1} at MC1, 0.08 ± 0.04 mg L^{-1} at MC2, 0.07 ± 0.04 mg L^{-1} at MC3, 0.05 ± 0.05 mg L^{-1} at SC1, and 0.03 ± 0.01 mg L^{-1} at P1 (Table 4, Figure 6B).

DON concentrations were generally higher in floodplain water than along the main channel, with averages of 0.20 ± 0.18 mg L^{-1} at SC1 and 0.12 ± 0.05 mg L^{-1} at P1, compared to 0.09 ± 0.04 mg L^{-1} at MC1, 0.10 ± 0.07 mg L^{-1} at MC2, and 0.10 ± 0.05 at MC3 (Table 4, Figure 6C). DON concentrations were similar at all sites from May – August but diverged during low flows; by late September, DON concentrations were over double as high at SC1, at 0.60 mg L^{-1}, than at any other location (Figure 6C).

Dissolved organic carbon (DOC) concentrations were relatively high at all locations during the May time period as the hydrograph began to rise (Figure 6D). As the hydrograph rose in response to snowmelt, DOC concentrations increased and peaked on the rising limb of the seasonal snowmelt hydrograph (Figure 6D). DOC concentrations began decreasing prior to peak flows and subsequently fell with the falling limb of the hydrograph. There was one peak in DOC at P1 associated with an early July rain event, but otherwise DOC generally declined on the hydrograph falling limb until early August (Figure 6D). However, DOC concentrations rose strongly in SC1 during the August – October time frame with a peak of 6.94 mg L^{-1} on September 28th (Figure 6D). Main channel average DOC concentrations across the study period were 3.50 ± 2.05 mg L^{-1} at MC1, 2.95 ± 1.87 mg L^{-1} at MC2, and 3.56 ± 1.81 mg L^{-1} at MC3, while floodplain DOC averages were 4.74 ± 1.71 mg L^{-1} at SC1 and 3.24 ± 1.81 mg L^{-1} at P1 (Table 4).

DOC measured from weekly grab samples was strongly correlated with simultaneous cDOM values (r^2 = 0.98, n = 32, Figure 7). Using the derived relationship in equation 7:

Eq. 7) $$[DOC] = 35.20[cDOM]^{0.98}$$

we transformed cDOM data to continuous DOC to calculate daily DOC fluxes at the main channel sites (Figure 8C), and daily and cumulative flux balances for the confined and unconfined segments (Figures 9C, 9F). Additionally, we calculated NO_3^-N and DON main channel fluxes (Figures 8A, 8B) and daily and cumulative flux balances (Figures 9A, 9B, 9D, and 9E) from grab samples. Main channel NO_3-N, DON and DOC fluxes followed the hydrograph (Figure 8). Maximum daily fluxes were between 5.6 – 8.0 g NO_3-N ha^{-1}, 5.7 – 8.7 g DON ha^{-1}, and 230 – 360 g DOC ha^{-1} during the high flow period from June 4th – 22nd (Figure 8), declined with runoff, and stabilized at values below 0.5 g NO_3-N ha^{-1}, 0.9 g DON ha^{-1} and 30 g

DOC ha^{-1} by August 1st (Figure 8). MC1 generally had lower daily nutrient fluxes than the other two main channel sites, and averaged 1.79 ± 1.94 g NO_3-N ha^{-1}, 1.75 ± 2.00 g DON ha^{-1} and 79.8 ± 73.5 g DOC ha^{-1} (Table 5, Figure 8). Mean daily solute fluxes at MC2 and MC3 were more similar to one another, and averaged 2.49 ± 2.88 g NO_3-N ha^{-1}, 2.63 ± 2.74 g DON ha^{-1} and 84.9 ± 94.4 g DOC ha^{-1} at MC2, and 2.27 ± 2.47 g NO_3-N ha^{-1}, 2.55 ± 1.85 g DON ha^{-1} and 86 ± 81 g DOC ha^{-1} at MC3 (Table 5, Figure 8). MC2, the outflow of the confined segment, had lower overall variability in daily solute fluxes than MC3, the outflow of the unconfined segment (Table 5, Figure 8).

Daily and cumulative flux balances for each segment highlight the ability of the unconfined segment to retain DOC and N relative to the confined segment (Figure 9). While the confined segment was a consistent source (net exporter) of dissolved carbon and nutrients, the unconfined segment displayed variable source-sink dynamics, exporting DOC and N during low flows and storing the solutes during high flows (Figure 9). From May – October the confined segment exported 26 g NO_3-N ha^{-1}, 41 g DON ha^{-1} and 721 g DOC ha^{-1}, whereas the unconfined segment stored 1.2 g NO_3-N ha^{-1} and 1.8 g DON ha^{-1} and exported only 7.7 g DOC ha^{-1} for every 100 m of river length (Figure 9). Accordingly, the unconfined segment was a slight sink for N and a slight source for C at this timescale. Notably, for any given downstream length, the unconfined segment retained ~99% of the upstream contribution of DOC (Data: net export from confined = 721 g DOC ha^{-1}; net export from unconfined = 8 g DOC ha^{-1}) and greater than 100% of the upstream contribution of NO_3-N (Figure 9).

3.3. Dissolved oxygen and fluvial ecosystem metabolism

At all locations, dissolved oxygen (DO) data negatively correlated with mean daily temperatures. Accordingly, the hourly rates of change in observed DO concentrations tended to

be more positive during the cooler night hours than warmer daylight hours. These results were counter to what we would have expected if only ER or GPP influenced the shape of the diel DO curves, and required that we corrected the hourly rate of DO change data for atmospheric exchange (see Eq. 1). Under all scenarios in which we calculated reaeration (Supplemental Table 1), the hourly rates of DO change corrected for atmospheric exchange became more positive during daylight than night hours, which was closer to what we would expect if only GPP and ER were influencing hourly rates of DO change. The shift to more positive hourly rates of DO change during daylight than night hours was predominantly attributed to the inclusion of average O_2 saturation deficit or excess in the atmospheric exchange equation, which should theoretically negate the influence of temperature on the shape of the diel DO curve. Calculating atmospheric exchange under different reaeration scenarios (Supplemental Table 1) suggested that correcting the reaeration coefficient for temperature (Eq. 4) made very little difference in the calculated metabolism metrics at all sites (Supplemental Figure 1). However, these same data indicate that changes in water velocity from May – October influenced the results at some sites more than others; for example, metabolism metrics at SC1 were highly sensitive to changes in water velocities whereas metrics at P1 exhibited little differences depending on the wind speed that we used to calculated reaeration (Supplemental Figure 1).

Gross primary productivity (GPP) and ecosystem respiration (ER) rates were strongly correlated with one another at each site (Figure 10). MC2, the confined outflow, generally had the lowest and most consistent metabolic processing rates of all sites, with an average GPP of $+0.09 \pm 0.14$ g O_2 m^2 d^{-1} and an average ER of -0.72 ± 0.50 g O_2 m^2 d^{-1} (Table 6, Figure 10). At MC2, GPP rates were relatively insensitive to changes in runoff, while ER increased during the snowmelt peak and July 7^{th} – 9^{th} storm (Figure 10). MC3, the unconfined outflow, had higher

and more variable metabolism rates than MC2, with an average GPP of +1.01 ± 0.76 g O_2 m^2 d^{-1} and an average ER of -1.77 ± 1.10 g O_2 m^2 d^{-1} (Table 6, Figure 10). Metabolism at MC3 generally had the opposite trend with runoff than at MC2, as GPP and ER rates were lowest during the snowmelt peak and increased as the hydrograph receded to baseflow, reaching a maximum of +2.88 g O_2 m^2 d^{-1} GPP on September 18th and -3.96 g O_2 m^2 d^{-1} ER on September 21st (Figure 10). While metabolic processing at MC3 generally increased from peak snowmelt to baseflow, GPP and ER rates decreased by >1 g O_2 m^2 d^{-1} during the last week of monitoring in late September (Figure 10).

Within the floodplain water-bodies, the side-channel (SC1) and pond (P1), metabolism generally increased as the hydrograph receded (Figure 10). Of the floodplain water-bodies, SC1 had the highest metabolism rates with an average GPP of +0.93 ± 0.50 g O_2 m^2 d^{-1} and an average ER of -2.64 ± 1.00 g O_2 m^2 d^{-1} (Table 6, Figure 10). While the average GPP rate at SC1 was slightly less than the maximum average observed for all sites (+1.01 ± 0.76 g O_2 m^2 d^{-1} at MC3), the average ER rate was substantially higher than any of the other sites (Table 6, Figure 11). The high average ER rate at SC1 was largely attributed to the peak in values between -4.32 and -5.04 g O_2 m^2 d^{-1} from August 14th –20th (Figure 10). Compared to SC1, P1 had lower and less variable metabolic processing rates, with an average GPP of +0.57 ± 0.33 g O_2 m^2 d^{-1} and an average ER of -0.56 ± 0.32 g O_2 m^2 d^{-1} over the monitoring period (Table 6, Figure 10). P1 metabolism generally increased as the hydrograph receded but remained within a moderate range, reaching a maximum GPP of only +1.31 g O_2 m^2 d^{-1} and a maximum ER of only -1.33 g O_2 m^2 d^{-1} in late September (Figure 10).

From May – October, average net ecosystem productivity (NEP) rates were negative (heterotrophic) along the main channel and side-channel and positive (autotrophic) in the pond

(Table 6, Figure 11). The main channel was strongly heterotrophic; MC2 NEP rates averaged -0.63 ± 0.44 g O_2 m^2 d^{-1} and were negative for all of the days that we monitored except July 5th, and MC3 NEP rates averaged -0.76 ± 0.48 g O_2 m^2 d^{-1} and were negative for 91% of the days we monitored (Figure 11). Trends in NEP rates contrasted between the confined and unconfined river segments; for example, during peak snowmelt, MC2 rates were the most negative and MC3 rates were the most positive (Figure 11). NEP rates also contrasted between floodplain water-bodies, and were the most negative and variable in SC1, at -1.70 ± 0.8 g O_2 m^2 d^{-1} , and the most positive and consistent in P1, at +0.01 ± 0.09 g O_2 m^2 d^{-1} (Table 6, Figure 11). SC1 became increasingly heterotrophic until August 14th, when the trend reversed (Figure 11), whereas P1 NEP rates were stable throughout the monitoring period.

4. DISCUSSION

From May – October 2015, we evaluated relationships between: (1) lateral hydrologic connectivity; (2) water, carbon, and nutrient flux; and (3) ecosystem metabolism in a confined and an adjacent (directly downstream) unconfined segment of North Saint Vrain Creek in Rocky Mountain National Park, Colorado. We calculated segment flux balances for water, carbon, and nitrogen at main channel sites MC1, MC2, and MC3, in which MC1 and MC2 bracket the confined segment, and MC2 and MC3 bracket the unconfined segment (Figure 1). We quantified ecosystem metabolism for the confined and unconfined main channel segments and in two floodplain water-bodies; an intermittently surface connected side-channel (SC1) and a subsurface connected pond (P1) (Figure 1). Main channel metabolism was measured at the outflow of the confined segment (MC2) and at the outflow of the unconfined segment (MC3) (Figure 1). Using these data, we asked the following questions: 1) *How do water, nitrogen, and carbon fluxes vary between a confined and unconfined river segment within the same network?*; and 2) *How does ecosystem metabolism and associated nutrient processing vary as a function of lateral connectivity?*

4.1 How do water, nitrogen, and carbon fluxes vary between a confined and unconfined river segment within the same network?

Variations in channel confinement control how different river segments respond to high flows (Montgomery and Buffington 1997, Bellmore and Baxter 2014) and can presumably influence the timing and magnitude of hydrologic and biogeochemical fluxes in river networks. During high flows, unconfined rivers reduce stream power by dissipating flow laterally across the floodplain, whereas rivers that are valley-constrained respond to increased discharge by

increasing water velocity and depth (Montgomery and Buffington 1997). Accordingly, the confined segment of North Saint Vrain Creek was a net source (exporter) of water from May – October, and for every 100 m of river length, exported 14.4 mm of water compared to the only 1.1 mm of water exported by the unconfined segment located directly downstream (Figure 4). Although the unconfined segment was a cumulative net source of water for the entire monitoring period, it exhibited variable hydrologic source-sink dynamics during the season as a function of runoff. The unconfined segment was a sink when flows exceeded ~4 mm d^{-1} on the rising limb, and remained a sink until flows dropped below ~2 mm d^{-1} on the falling limb of the seasonal snowmelt hydrograph (Figure 12A). Hydrologic source-sink dynamics in unconfined river segments are strongly linked to the physical and chemical spatiotemporal heterogeneity of the floodplain riverscape (Junk et al. 1989, Malard et al. 2000). Over time, the lateral redistribution of water during high flows can scour the floodplain and create a network of diverse fluvial habitats (side-channels, ponds, oxbow lakes), with increased opportunities for surface water storage (Junk et al. 1989). Water stored in these fluvial habitats can readily infiltrate to the subsurface and create larger hyporheic zones relative to those located in more confined river segments (Stanford and Ward 1993, Montgomery and Buffington 1997). During low flow periods, floodplains have been demonstrated to release subsurface water stored during high flow periods back to the river (Mertes 1997).

In river-floodplain systems, the lateral redistribution of water during high flows can deliver dissolved carbon and nutrients to floodplain water-bodies where it can be physically and biologically retained (Tockner et al. 1999). Accordingly, DOC and N retention along the unconfined segment was strongly related to hydrologic source-sink dynamics (Figures 4, 9). The unconfined segment functioned as a sink for N at all flows above 2 mm d^{-1}, and a DOC sink

when flows exceeded ~4 mm d^{-1} on the rising limb of the hydrograph (Figures 12B, 12C). When the hydrograph fell below ~2 mm d^{-1} on the falling limb, the unconfined segment transitioned from a sink to a source for DOC (Figure 12C). During low flows, high rates of floodplain GPP (Figure 10) suggest that the DOC exported to the river from the floodplain was largely derived from autochthonous production, and therefore more labile than allochthonous DOC (Wiegner et al. 2005). Because labile organic matter can enhance downstream microbial decomposition and N and phosphorous (P) cycling (Aerts 1997), the net export of DOC along the unconfined segment may have contributed to the enhanced microbial respiration during low flows.

While metabolism rates were higher along the unconfined compared to the confined segment, metabolism rates alone are insufficient to explain all of the DOC and N retention observed along the unconfined segment. Over 99% of the incoming DOC and over 100% of the incoming N were retained from the upstream confined segment from May – October (Figure 9), yet the unconfined segment had only 0.92 g O_2 m^2 d^{-1} higher GPP and 1.05 g O_2 m^2 d^{-1} higher ER on average than the confined segment (Table 6, Figure 10). The discrepancy between DOC and N retention and associated metabolism rates along each segment can largely be attributed to the differences in the size of the active fluvial areas between segments. We calculated the active fluvial area of the unconfined segment to be ~120,000 m^2 (data: unconfined segment valley bottom area as determined in GIS is ~480,000 m^2, with ~25% inundated by water during peak snowmelt), and the active area of the confined segment to be 3000 m^2 (data: confined segment valley bottom area as determined in GIS is ~3000 m^2). These data suggest that the unconfined segment valley-bottom has an active area that is approximately 40 times larger than the active area of the confined segment. Further, geomorphic and hydraulic complexity, prevalent in dynamic river-floodplain systems, has been demonstrated to enhance dissolved matter retention

by increased opportunities for nutrient uptake (Lamberti et al. 1989), microbial transformations (e.g., denitrification) (Hill et al. 1998), and physical sorption onto substrates (McKnight et al. 1992). Combined, these factors likely influenced the particularly high rates of DOC and N retention along the unconfined relative to the confined segment.

Beaver (*Castor canadensis)* activity along the unconfined segment contributed to enhanced water, DOC, and N retention in the unconfined segment through the construction of multiple beaver dams and ponds. By raising local water levels, beaver ponds can enhance hyporheic exchange (Westbrook et al. 2006) which can promote increased rates of anaerobic biogeochemical cycling and associated N removal by denitrification (Correll et al. 2000). However, much of the research that aims to establish linkages between beaver activity and carbon and nutrient retention focuses on the scale of individual beaver dam-pond pairs rather than the scale of the multi-thread, riparian wetland (e.g., "beaver meadow") that is created following the breaching of numerous beaver dams (Burchsted et al. 2010). To estimate annual DOC and N fluxes for the unconfined segment beaver meadow, we extrapolated daily fluxes over the missing time interval (September 29th 2015 – April 30th 2016) with the assumption that the fluxes on April 30th 2016 were equal to those on May 1st 2015, and summed all of the daily fluxes for the year to derive annual totals. We found that the unconfined beaver meadow retained net totals of 0.2 kg NO_3-N ha^{-1} yr^{-1} and 0.2 kg DON ha^{-1} yr^{-1} and exported a net total of 6.6 kg DOC ha^{-1} yr^{-1}. Normalized for area, the beaver meadow exported over ten times less DOC and retained over 10 times less NO_3-N compared to a beaver pond in the Adirondacks (Cirmo and Driscoll 1996), and exported over 100 times more NO_3-N than a beaver pond in the Maryland Coastal Plain (Correll et al. 2000). These data suggest that DOC and N flux balances derived for a single dam-pond pair may not necessarily scale up to the spatial unit of the beaver meadow,

although inter-site differences including variations in climate and hydrologic regimes (Devito et al. 1989) as well as the extent of watershed disturbance (Correll et al. 2000) must also be considered. Further, the limited number of grab samples we used to derive N fluxes introduced uncertainty in the data that was likely magnified when we extrapolated the data to derive annual totals.

The retention of water, DOC and N along unconfined valley bottoms can have important implications for hydrologic transport dynamics (Hey et al. 2012) and biogeochemical cycling (Cirmo and McDonnell 1997) in river networks. However, relative to their spatial extent, unconfined valley bottoms have been disproportionately altered by human practices such as grazing, flow regulation, and beaver trapping (Wohl 2001). By reducing lateral hydrologic connectivity (Hupp et al. 2009), these practices may exacerbate the societal and ecological consequences associated with climate change forecasts and anthropogenic N pollution. For example, the increased potentials for drought and flooding in the Rocky Mountain region (Dominguez et al. 2012) and concerns over increased anthropogenic N input to fluvial networks (Vitousek et al. 1997) has created a growing need for retentive features that can attenuate flood pulses, release water during low flows, and process and remove N from the fluvial network. The contrasting export/retention dynamics of the confined and unconfined segments in our study emphasizes that unconfined valley bottoms can be important sites in controlling water, carbon, and nutrient dynamics along fluvial networks and may be critical features to protect and enhance in watershed management plans.

4.2 How does ecosystem metabolism and associated nutrient processing vary as a function of lateral connectivity?

Fluvial ecosystem metabolism can be influenced by numerous parameters including: light (González-Pinzón et al. 2016), temperature (Mulholland et al. 2001), nutrient supply (Roberts and Mulholland 2007), biomass (Bernot et al. 2010), and hydrology (Jones et al. 1995). We found lateral hydrologic connectivity dynamics from high to low flows exerted primary controls on the spatiotemporal trends in metabolism observed along the confined and unconfined segments and in individual floodplain water-bodies. While other studies have cited temperature and light intensity as potential controls on GPP and ER (Sinsabaugh et al. 1994, Hill et al. 1995, Lamberti and Steinman 1997, Mulholland et al. 2001), we observed no significant ($p > 0.05$) relationships between temperature and metabolism metrics along either the confined or unconfined river segments. Shifts in light intensity through time may have influenced seasonal variation in metabolism rates, although had it been the primary control on metabolism we would have expected to find more similar seasonal metabolism trends between sites in contrast to the distinct, and sometimes opposing, trends we observed through time (Figures 10, 11). Lateral hydrologic connectivity, by controlling spatiotemporal variability in hydrologic and biogeochemical retention (Figures 4, 9), can better explain the contrasting metabolism dynamics between the confined and unconfined segments from high to low flows.

4.2.1 Contrasting ecosystem metabolism dynamics along a confined and unconfined segment as a function of lateral connectivity

Lateral hydrologic connectivity, by controlling spatiotemporal variability in hydrologic and biogeochemical retention (Figures 4, 9), influenced the contrasting metabolism dynamics between the confined and unconfined segments from high to low flows. Compared to the unconfined segment, the confined segment had lower average metabolism rates (Table 6, Figure 10), as the consistent export of water, DOC, and N across flows (Figures 4, 9) and relatively

small active area likely reduced opportunities for microbial interactions with solutes (Battin et al. 2008). Lower metabolism rates, in turn, could have further increased the export of DOC and N. Conversely, along the unconfined segment, the lateral redistribution of flow, large active area, and associated retention of water, DOC, and N likely enhanced opportunities for metabolic processing. Accordingly, the unconfined segment had on average 0.92 g O_2 m^2 d^{-1} higher GPP and 1.05 g O_2 m^2 d^{-1} higher ER than the confined segment from May – October (Table 6, Figure 10). During high flows, the retention of water, DOC and N (Figures 4, 9) was probably predominantly associated with the physical process of overbank flooding as opposed to biological processing. GPP and ER rates in the main channel of the unconfined segment were lowest during this time (Figure 10), as high flows can depress metabolism by reducing residence times (Battin et al. 2008) and scouring biofilms (Fisher et al. 1982, Uehlinger and Naegeli 1998). Nevertheless, the delivery of water, DOC, and N along the floodplain during high flows presumably created the conditions for the high processing rates observed during subsequent low flow periods (Figure 10) by supplying resources (C, N) to slower moving floodplain water-bodies. The contribution of floodplain "hot spots" (McClain et al. 2003) to enhanced biogeochemical cycling generally increased as the hydrograph receded and residence times of the floodplain water-bodies increased. Accordingly, metabolism rates along the unconfined segment increased to a maximum GPP of +2.88 g O_2 m^2 d^{-1} on September 18th and a maximum ER of -3.96 g O_2 m^2 d^{-1} on September 21st (Figure 10). However, these rates each declined by >1 g O_2 m^{-2} d^{-1} during the last week of monitoring (Figure 10); which, corresponding with a near-total decrease in main channel NO_3-N concentrations (Figure 6B), were consistent with findings that inorganic nutrient availability can limit GPP (Peterson et al. 1985) and ER (Mulholland et al. 2001). Decreases in metabolic processing likely due to NO_3-N limitation also occurred at this

time in our monitored floodplain side-channel (SC1) (Figures 6B, 10), and potentially other intermittently surface connected water-bodies along the floodplain as well. As such, these sites would have no longer acted as biogeochemical "hot spots" nor strongly contributed to main channel biogeochemical cycling. Along the unconfined segment, metabolism was optimized at a trade-off between nutrient availability during high flows/high connectivity and increased residence times during low flows/low connectivity.

Lateral hydrologic connectivity also influenced net ecosystem productivity (NEP) dynamics across river segments (Figure 11). The main channel of both the confined and unconfined segments were predominantly heterotrophic (negative NEP) for the monitoring period, which is typical for low-order forested streams (Mulholland et al. 2001). However, trends in NEP with runoff differed between segments, as the confined segment had the most negative NEP rates during peak snowmelt whereas the unconfined segment had the least negative NEP rates during peak snowmelt (Figure 11). The contrasting NEP dynamics across river segments was likely related to differences in DOC export dynamics between segments. In contrast to the confined segment, the unconfined segment transitioned from a net sink to a net source of DOC from high to low flows (Figure 12C). The export of floodplain DOC during low flows related to simultaneously high floodplain GPP rates (Figure 10A), which suggests that the DOC pool consisted of more labile molecules than those of allochthonous origin (Wiegner et al. 2005) and may have stimulated downstream microbial respiration (Aerts 1997). Additionally, the shift along the unconfined segment from a net sink to a net source of water as the hydrograph receded suggests that the segment floodplain had a substantial groundwater or hyporheic area during the low flow period capable of maintaining downstream water supply. The lateral redistribution of flow has been demonstrated to expand and create much larger hyporheic zones in unconfined

versus confined segments (Stanford and Ward 1993), and these zones can be hot spots for microbial respiration and associated heterotrophy (Fellows et al. 2001). Lateral hydrologic connectivity, by delivering labile DOC from the floodplain to the river (Junk et al. 1989, Ward and Stanford 1995) and expanding the size of the hyporheic zone (Stanford and Ward 1993) may have resulted in higher heterotrophy on average along the unconfined than the confined river segment (Table 6, Figure 11).

4.2.2 Contrasting ecosystem metabolism dynamics in floodplain surface water-bodies as a function of lateral connectivity

Shifts in the strength and type (e.g., surface, subsurface) of river-floodplain connectivity can have important implications for the structural and functional characteristics of the floodplain (Tockner et al. 1999). We found that within floodplain surface water-bodies, intermittent surface water connectivity with the main channel, by controlling water velocity and the delivery of metabolic resources (e.g., C, N), resulted in highly dynamic ecosystems with enhanced biogeochemical cycling. The distinct metabolism dynamics between the side-channel (SC1) and pond (P1) (Figure 10) reflected the unique roles of intermittent surface versus subsurface connectivity, respectively, on biogeochemical processing. From May – October, SC1 had on average 0.36 g O_2 m^2 d^{-1} higher GPP and 2.08 g O_2 m^2 d^{-1} higher ER than P1 (Table 6, Figure 10). The slight increase in GPP rates from high to low flows were similar at both sites (Figure 10A), while trends in ER were distinct between sites, with the largest rates and greatest variabilities observed at SC1 (Table 6, Figure 10B). While we are unware of any study to date that relates changes in ER to shifts in the strength of river-floodplain connectivity, several studies have established relationships between ER rates and the hydrologic dynamics of storm events (Uehlinger and Naegeli 1998, Uehlinger 2000, 2006, Roberts and Mulholland 2007),

which may be considered analogous. In a forested headwater stream in Tennessee, Roberts and Mulholland 2007 found that while storms initially depressed ER, the storms stimulated ER rates to nearly triple pre-storm levels over the subsequent days (Roberts and Mulholland 2007). The authors attributed the post-storm increase in ER primarily to the deposition of labile organic matter from the catchment during the storm (Roberts and Mulholland 2007). While operating at larger spatial and temporal scales than a single storm event, overbank flooding during peak runoff in dynamic river-floodplain systems may have similar influences on processing rates. Overbank flooding may initially depress ER rates in intermittently connected floodplain water-bodies (e.g., SC1; Figure 10B) by reducing residence times and increasing scour, while enhancing ER during subsequent low flow periods by delivering large quantities of organic carbon and nutrients (N, P) (Roberts and Mulholland 2007). Accordingly, during peak snowmelt in June, resource supplies at SC1 were relatively high – at 5.9 mg DOC L^{-1} and 0.15 mg NO_3-N L^{-1} (Figures 6B, 6D) – while ER rates remained under -2.16 g O_2 m^{-2} d^{-1} (Figure 10B). Following surface water disconnection with the main channel in mid-July (Table 3, Figure 5), SC1 ER rates increased substantially to the maximum rate observed for all sites, -5.04 g O_2 m^{-2} d^{-1}, on August 17th (Figure 10B).

During the low flow/low connectivity period, increased metabolic processing at SC1 was associated with high DOC (6.9 mg L^{-1}) and DON (0.60 mg L^{-1}**)** concentrations, along with a strong depletion of NO_3-N (Figures 6B, 6C, 6D). High DON and DOC concentrations during low flows at SC1 suggests high biologic productivity and associated nutrient demand, consistent with the simultaneously low NO_3-N concentrations (Figure 6B). As the NO_3-N supply became exhausted at SC1 in August, metabolism declined by ~0.5 g O_2 m^{-2} d^{-1} GPP and ~-2 g O_2 m^{-2} d^{-1} ER (Figure 10). Following lateral hydrologic disconnection with the main channel, SC1

residence times and associated metabolic processing increased (Figure 10), which likely increased autochthonous production of organic matter (DOC, DON) (Figures 6C, 6D) until the majority of NO_3-N had been assimilated (Figure 6B), the aquatic ecosystem became nutrient limited, and metabolic processing decreased (Figure 10). While the surface water disconnection of floodplain water-bodies can be crucial to increase residence times and associated metabolic processing, episodic surface water connection is likely required to replenish important nutrient stocks and maintain high rates of metabolic processing.

Compared to the intermittently surface connected side-channel, our intensively studied pond (P1) never became surface-connected to the main channel and had average water velocities consistently at or close to 0 cm s^{-1} for the duration of the monitoring period. Related to stable hydrologic conditions at P1, metabolism rates were much less variable at P1 than at SC1 (Table 6, Figures 10, 11), and the slight increases in metabolic processing from May – October (Figure 10) were more likely attributed to shifts in subsurface resource supply (e.g., Tockner et al. 1999) and sediment hypoxia (e.g., Lazar et al. 2015) rather than changes in residence times associated with variable flow rates. While organic matter concentrations increased in P1 during the high flow/high connectivity period in early June (Figures 6C, 6D), the delivery of organic matter from subsurface flow paths would have been limited to the dissolved constituents only (Tockner et al. 1999), and the lack of particulate organic matter may explain in part why metabolism rates at P1 never reached the magnitudes observed at SC1 (Table 6, Figure 10). With no outlet or scouring events, biological detritus would have continually accumulated onto an undisturbed layer of hypoxic bottom sediments as the season progressed. Decomposition of this detritus and the hypoxic inhibition of nitrification may explain why P1 NH_4-N concentrations, at 0.2 mg L^{-1} by late September, were substantially higher than at any of the other sites monitored (Figure 6A). At

P1, subsurface hydrologic exchanges likely contributed some dissolved matter to the site to stimulate metabolic processing throughout the season (Figures 6, 10); however, because P1 did not exhibit the same variability in residence times, nor receive a similar resource supply from the main channel as SC1, processing rates were much more stable at P1 than SC1 (Table 6, Figure 10).

Within floodplain water-bodies, the strength and type of lateral connectivity also influenced net ecosystem production (NEP) rates (Table 6, Figure 11). From May – October, SC1 had the greatest variability in NEP of all sites, with a standard deviation of +0.80 g O_2 m^2 d^{-1} which was nearly double the standard deviation of the next most variable site (Table 6, Figure 11). Conversely, P1 exhibited the most stable range in NEP rates across flows for all sites (Table 6, Figure 11). The slight autotrophic conditions observed at P1 is typical in lentic environments where photosynthetic organisms can more frequently develop without being scoured (Allan and Castillo 2007). However, SC1 generally exhibited the reverse effect, and became increasingly heterotrophic as it transitioned from lotic to lentic conditions until mid- to late- August (Figure 11). Increased organic matter input from flooding as well as later season leaf fall may have stimulated ER at greater rates than GPP and created heterotrophic conditions during mid-August at SC1. Further, data on post-storm recovery of ecosystem processing suggest that ER can recover more strongly than GPP from floods due to the resiliency of the hyporheic zone, in which a high portion of heterotrophic respiration can occur (Uehlinger and Naegeli 1998). In floodplain water-bodies of unconfined river segments, intermittent surface connections with the main channel can result in aquatic ecosystems with highly variable metabolic processing dynamics across flows.

5. CONCLUSIONS

We found that along two distinct segments of North Saint Vrain Creek, Colorado, lateral hydrologic connectivity controlled water, DOC and N retention, which in turn, influenced spatiotemporal patterns in fluvial ecosystem metabolism. An unconfined segment retained large quantities of water, DOC and N relative to a confined segment of the same river network, particularly during higher flow periods when overbank flooding dissipated energy across the floodplain. Lateral hydrologic exchanges across the unconfined segment during high flows created a floodplain riverscape with high geomorphic and hydraulic complexity, which in turn, promoted retention across a large active area through increased opportunities for nutrient uptake, microbial transformation (e.g., denitrification), and physical sorption onto substrates. During high flows in dynamic river-floodplain systems, large valley-bottom areas and geomorphic and hydraulic complexity promotes the retention of water, DOC, and N, with strong implications for flood attenuation, drought mitigation, and biogeochemical cycling in the river network.

In river-floodplain systems, floodplain surface water-bodies can play an active role in enhanced metabolic processing. Differences in metabolism trends between a side-channel and pond across flows reflected the unique roles of lateral connectivity type (i.e., intermittent versus no surface-water exchange) with the main channel on biogeochemical cycling. In the intermittently surface connected side-channel, high variability in residence times and resource (C, N) delivery due to episodic surface water connections related to high averages and large variability in metabolic processing rates, particularly with respect to ER. We suggest that while low flow/low connectivity periods can enhance processing rates due to increased residence times, episodic overbank flooding is required to replenish resource supply in these environments.

Compared to the side-channel, more stable hydrologic conditions in the pond related to less variable metabolic processing rates, and water chemistry dynamics were more likely dominated by redox conditions. In dynamic river-floodplain systems, the strength and type of lateral hydrologic exchanges influences spatiotemporal patterns in fluvial ecosystem metabolism, yet remains a poorly understood topic in watershed science. We suggest that future research directions continue to establish relationships between lateral connectivity and ecosystem processing rates, so that river-floodplain exchanges be more meaningfully implemented in environmental practices that seek to promote healthy and sustainable aquatic ecosystems.

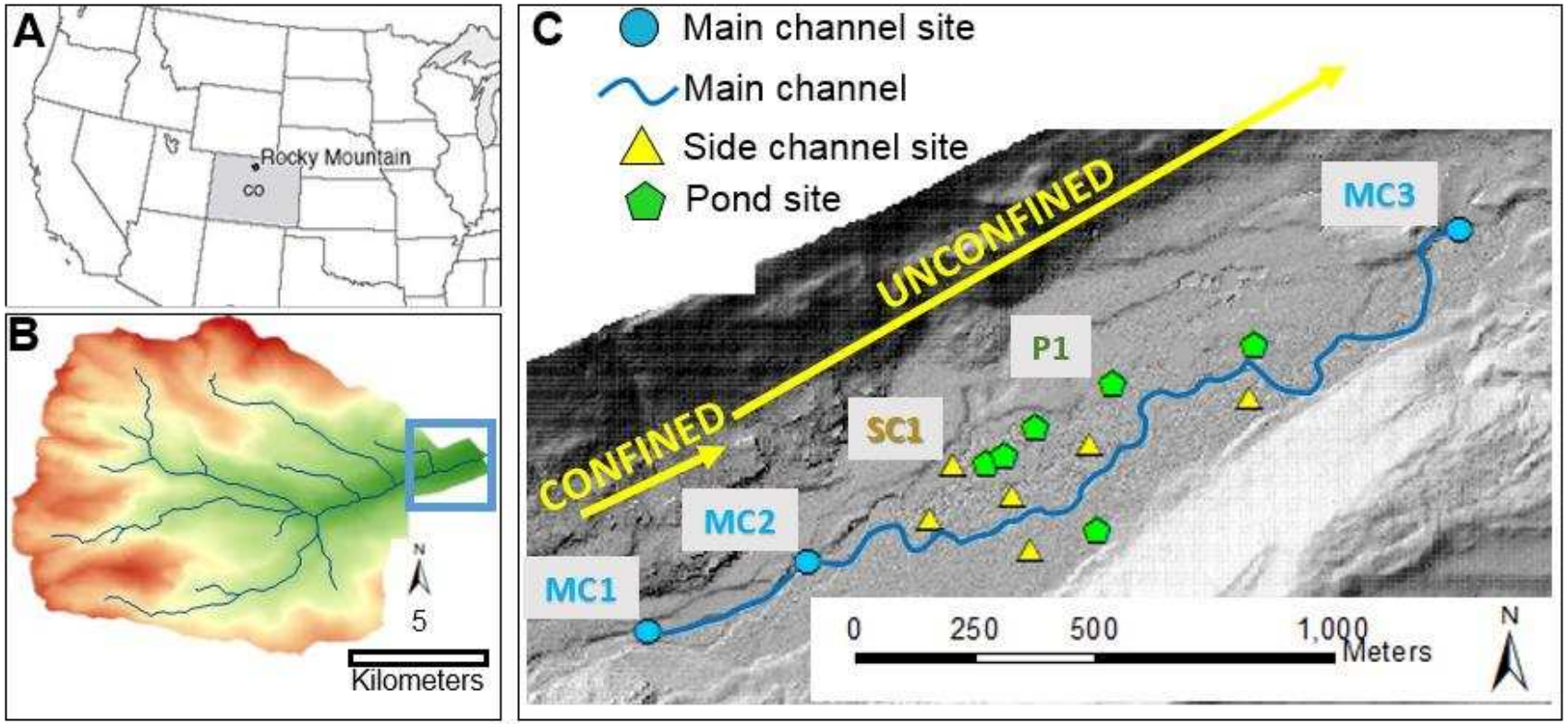

Figure 1. Maps showing a) Location of the Wild Basin Watershed in Colorado, b) Wild Basin Watershed with the study area highlighted in blue, and c) the confined and unconfined segments. We present metabolism data from three main channel sites (MC1, MC2, and MC3), a floodplain side-channel (SC1), and a floodplain pond (P1). MC1 and MC2 bracket the confined segment, and MC2 and MC3 bracket the unconfined segment.

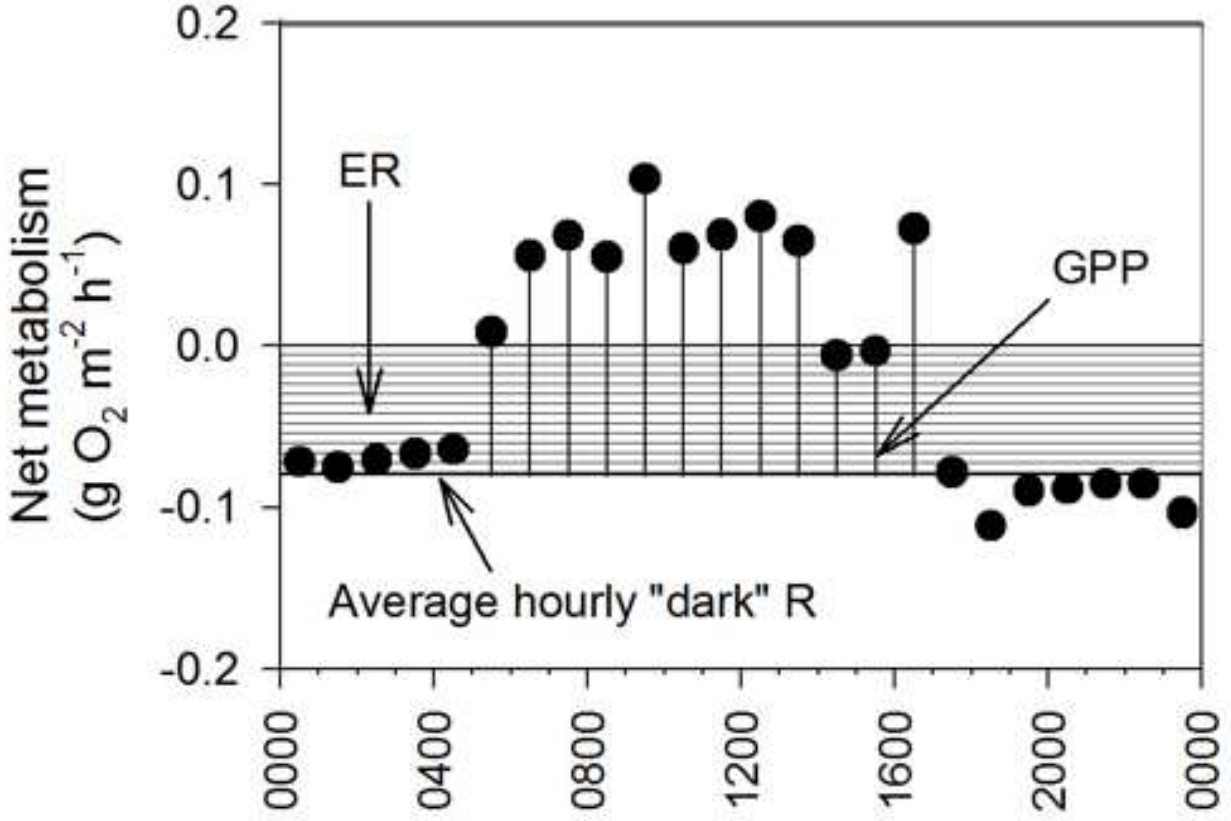

Figure 2. Hourly rates of dissolved oxygen (O_2) change corrected for atmospheric exchange on August 15th in the main channel (MC3). The bold horizontal line indicates the average hourly rate from post-sunset to pre-dawn, the area indicated by the horizontal lines represents ecosystem respiration (ER), and the area indicated by the vertical lines represents gross primary productivity (GPP).

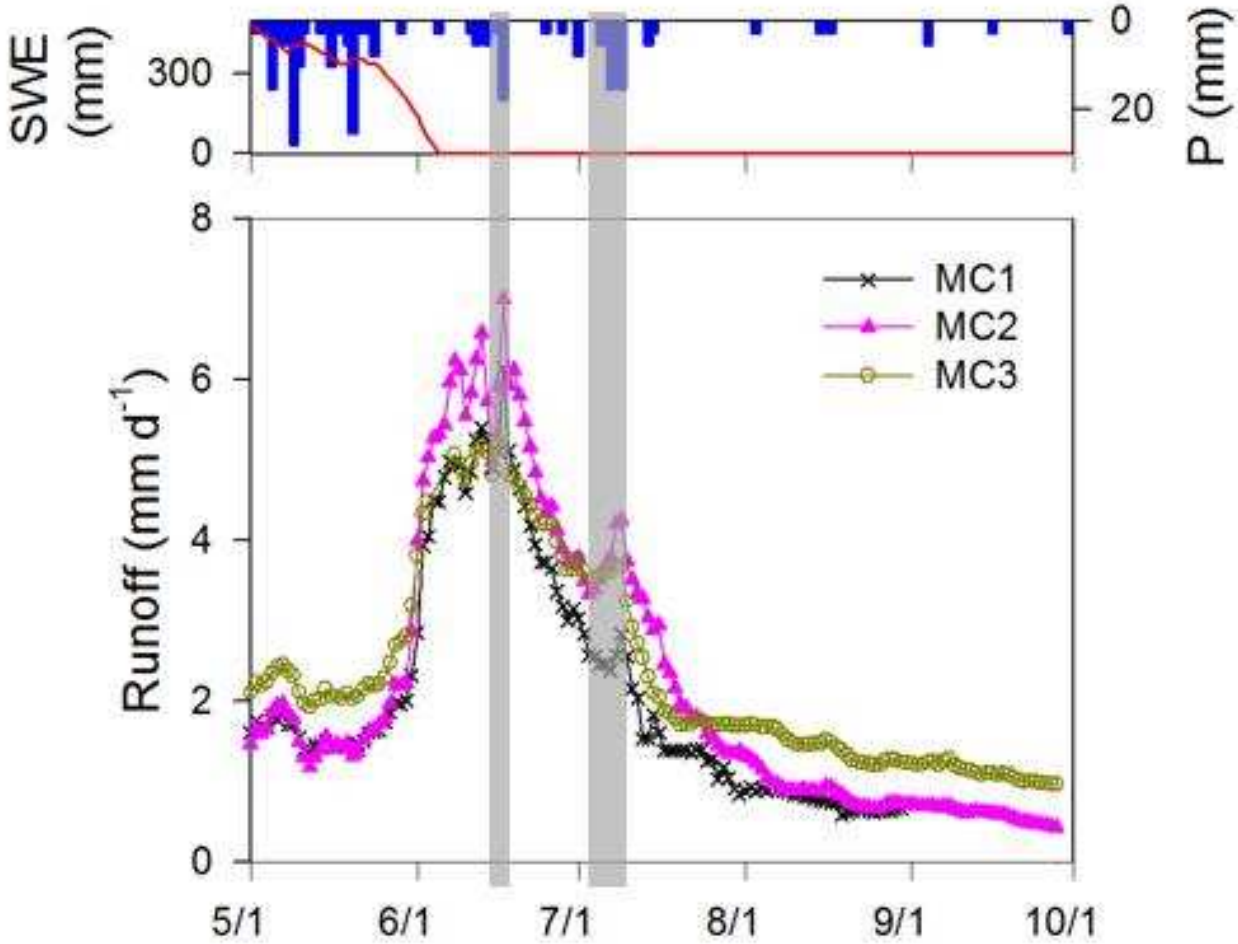

Figure 3. Precipitation (P) and snow water equivalent (SWE) with daily mean runoff at main channel sites MC1, MC2, and MC3. The confined segment is bracketed by MC1 and MC2, and the unconfined segment is bracketed by MC2 and MC3. Main channel runoff was predominantly driven by snowmelt, although runoff notably increased in response to the June 17th and July 7th – 9th storm events (shaded in gray).

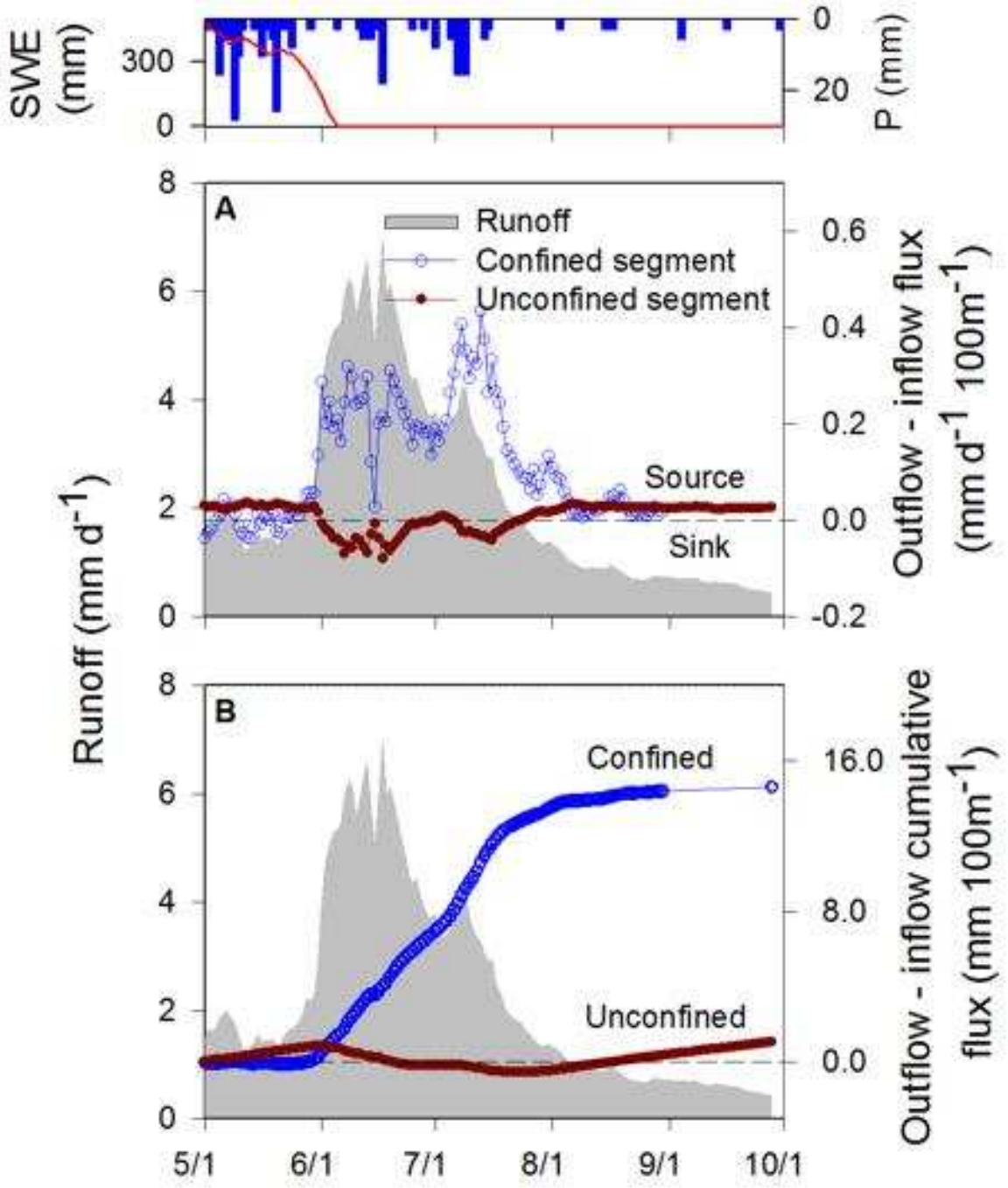

Figure 4. Precipitation (P) and snow water equivalent (SWE) and main channel runoff with daily and cumulative water flux balances per 100 m of river length. Over the monitoring period, the confined segment transported 14.4 mm $100m^{-1}$ of water, whereas the unconfined segment transported a net total of only 1.1 mm 100^{-1} of water.

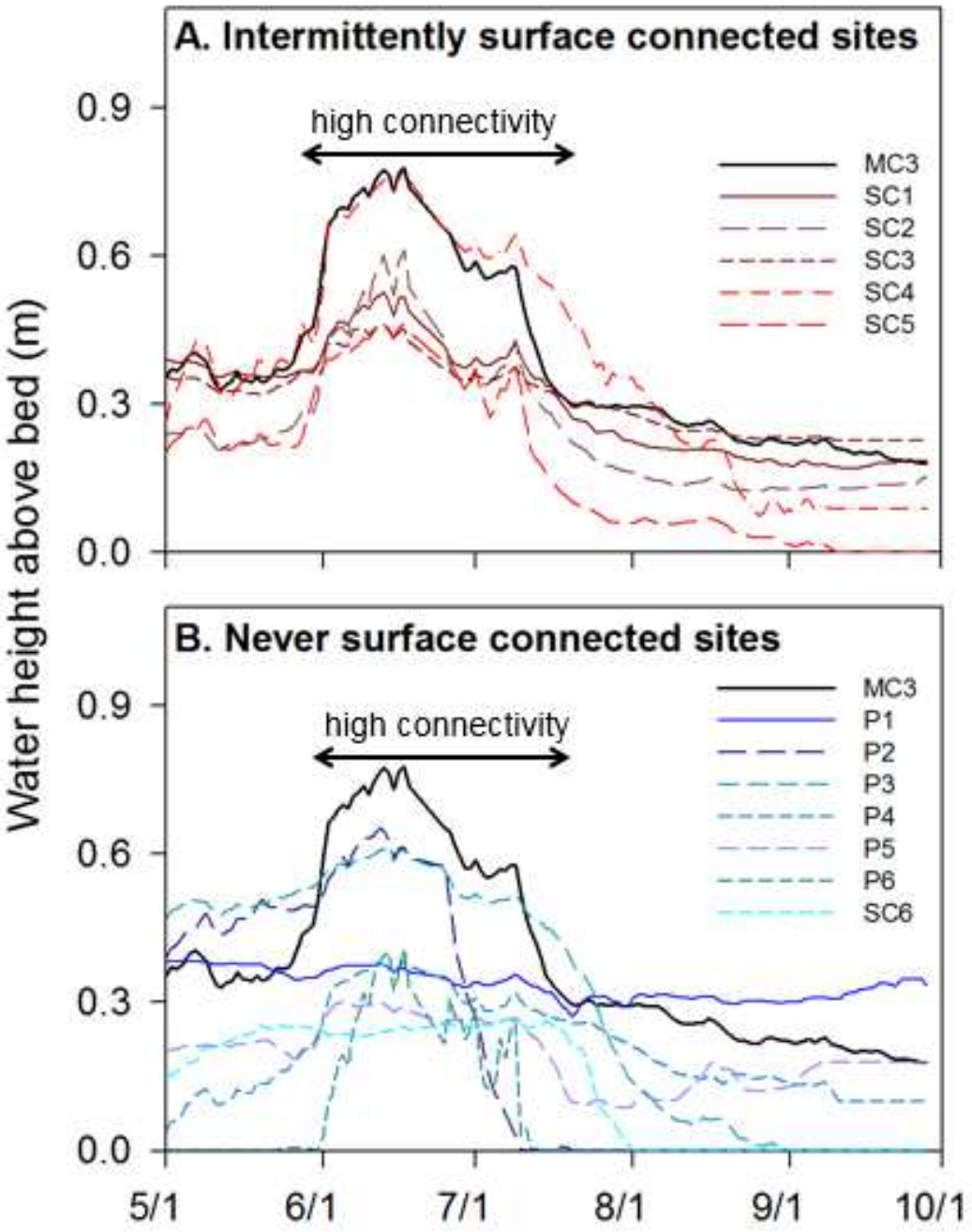

Figure 5. Water levels relative to the local ground elevation for the main channel (MC3) and floodplain side-channels and ponds with a) intermittent surface water connectivity, and b) no surface water connectivity with the main channel. For surface connected sites, high connectivity referred to the period of time in which the sites were hydrologically inundated by overbank flooding from the main channel. For sites with no surface water connectivity with the main channel, shifts in the strength of connectivity likely reflected transitions in subsurface hydrology. The majority of floodplain water-body sites exhibited high connectivity from late May until mid-July. Specific dates are listed in Table 3.

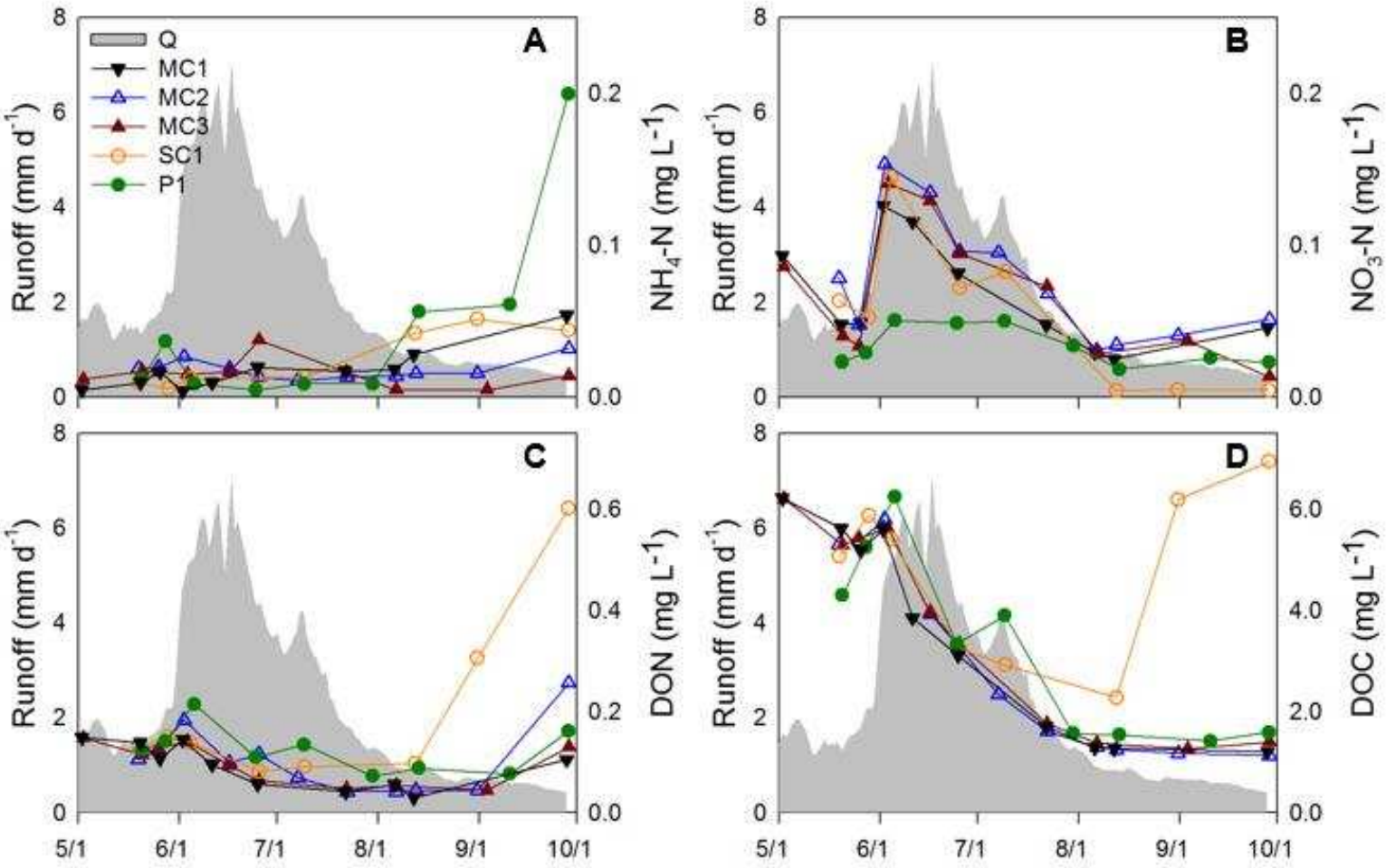

Figure 6. Dissolved nutrient concentrations at main channel monitoring sites MC1, MC2, and MC3, a floodplain side-channel, SC1, and pond, P1. Main-channel (MC2) runoff are presented with concentrations of a) nitrogen as ammonium (NH_4-N), b) nitrogen as nitrate (NO_3-N), c) dissolved organic nitrogen (DON), and d) dissolved organic carbon (DOC). Data are from grab samples taken approximately once every other week from May – October 2015.

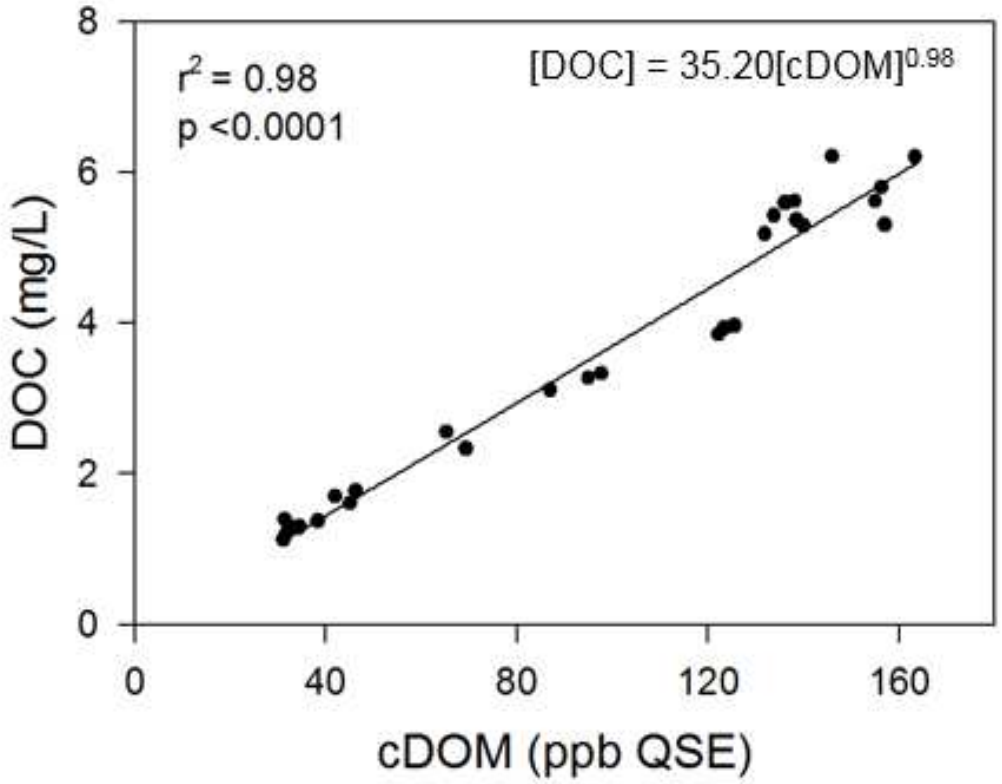

Figure 7. Relationship between dissolved organic carbon (DOC) analyzed from grab samples and simultaneous measurements of colored dissolved organic matter (cDOM) from a Turner Designs Inc. Cyclops 7 sensor in the main channel (n=30). The power regression curve was used to transform continuous cDOM measurements to a continuous DOC time series at MC1, MC2, and MC3. Data are from May – October 2015.

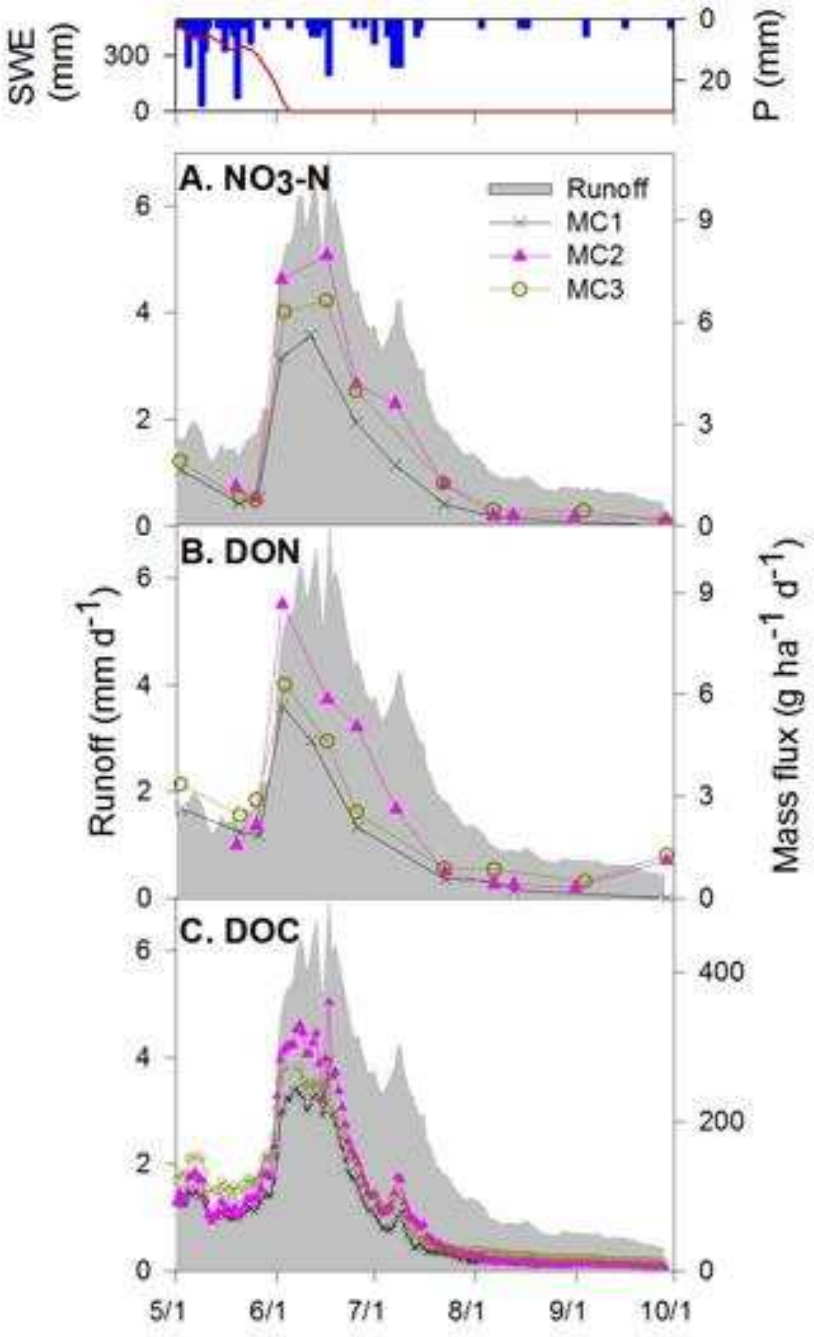

Figure 8. Precipitation (P) and snow water equivalent (SWE) and main channel (MC2) runoff with a) nitrate (NO_3-N), b) dissolved organic nitrogen (DON), and c) dissolved organic carbon (DOC) fluxes at main channel sites MC1, MC2, and MC3. The confined segment is bracketed by MC1 and MC2, and the unconfined segment is bracketed by MC2 and MC3. Daily fluxes are strongly correlated with main channel runoff.

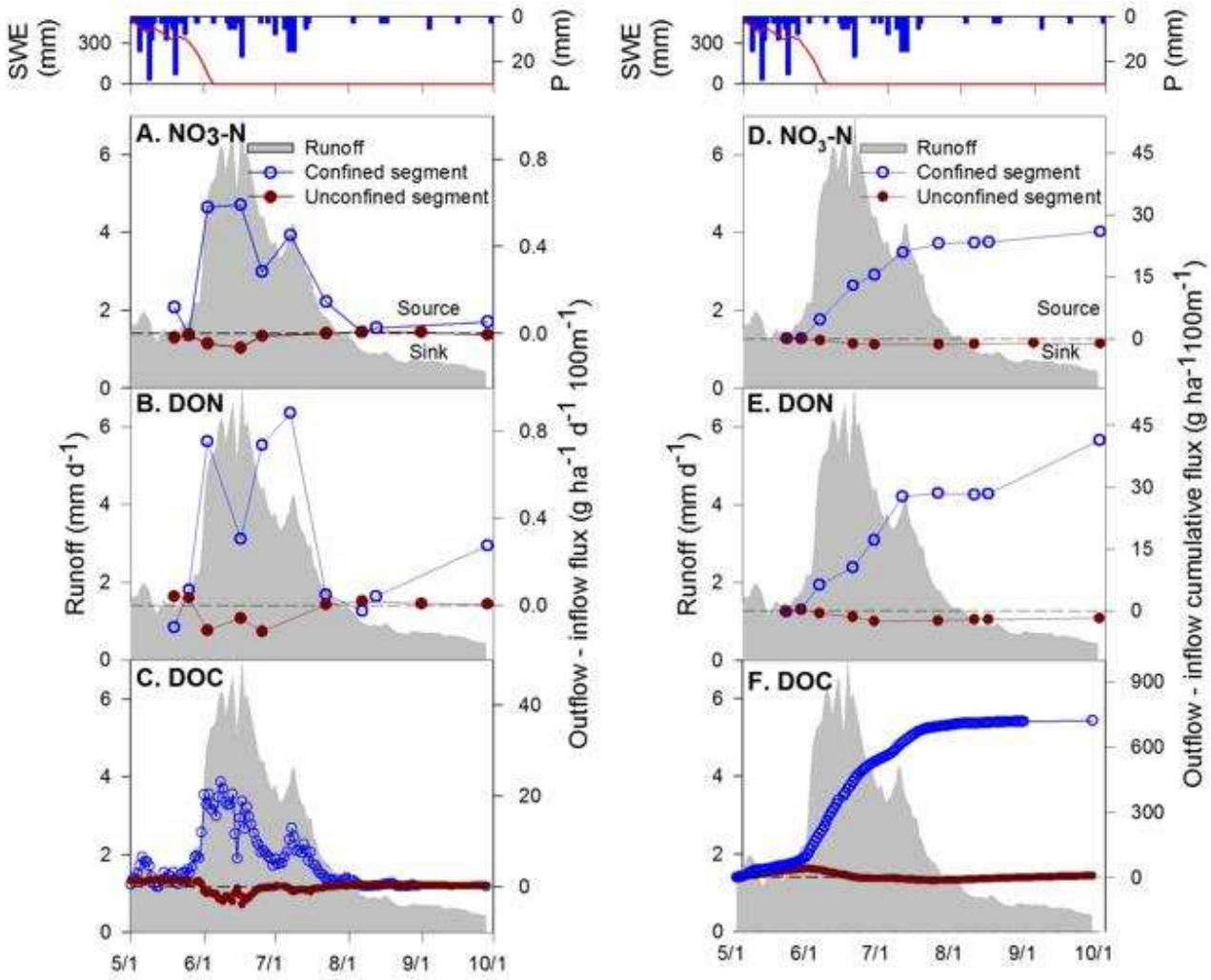

Figure 9. Precipitation (P) and snow water equivalent (SWE) and main channel (MC2) runoff with a) nitrate (NO_3-N), b) dissolved organic nitrogen (DON), and c) dissolved organic carbon (DOC) flux balances, and d) NO_3-N, e) DON, and f) DOC cumulative flux balances for the confined and unconfined segment per 100 m of river length. Over the monitoring period, the confined segment transported 26 g NO_3-N ha^{-1}, 41 g DON ha^{-1}, and 721 g DOC ha^{-1}, whereas the unconfined segment stored a net total of 1.2 g NO_3-N ha^{-1}, 1.8 g DON ha^{-1}, and transported a net total of only 7.7 g DOC ha^{-1} for every 100 meters of river length.

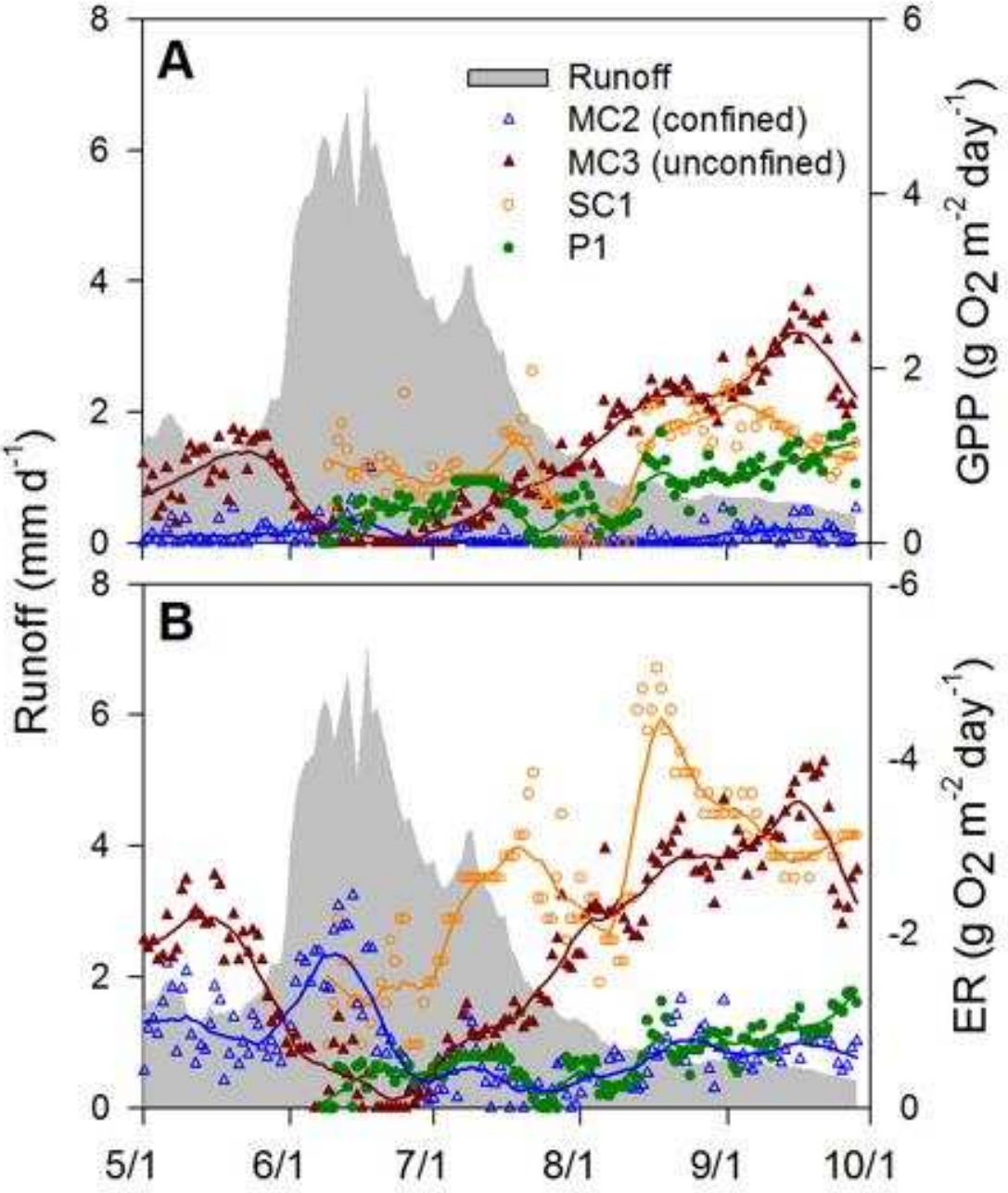

Figure 10. Main channel (MC2) runoff with a) Gross primary productivity (GPP), and b) ecosystem respiration (ER) at main channel sites MC2 (confined outflow) and MC3 (unconfined outflow), and a floodplain side-channel, SC1, and pond, P1. Metabolism metrics were calculated using an open system, single station dissolved oxygen approach. Main channel monitoring began on May 1st and floodplain water-body monitoring began on June 9th. GPP and ER measured at MC2 were consistently lower and less variable than those measured at MC3, and strong increases in ER occurred at SC1 as the hydrograph receded.

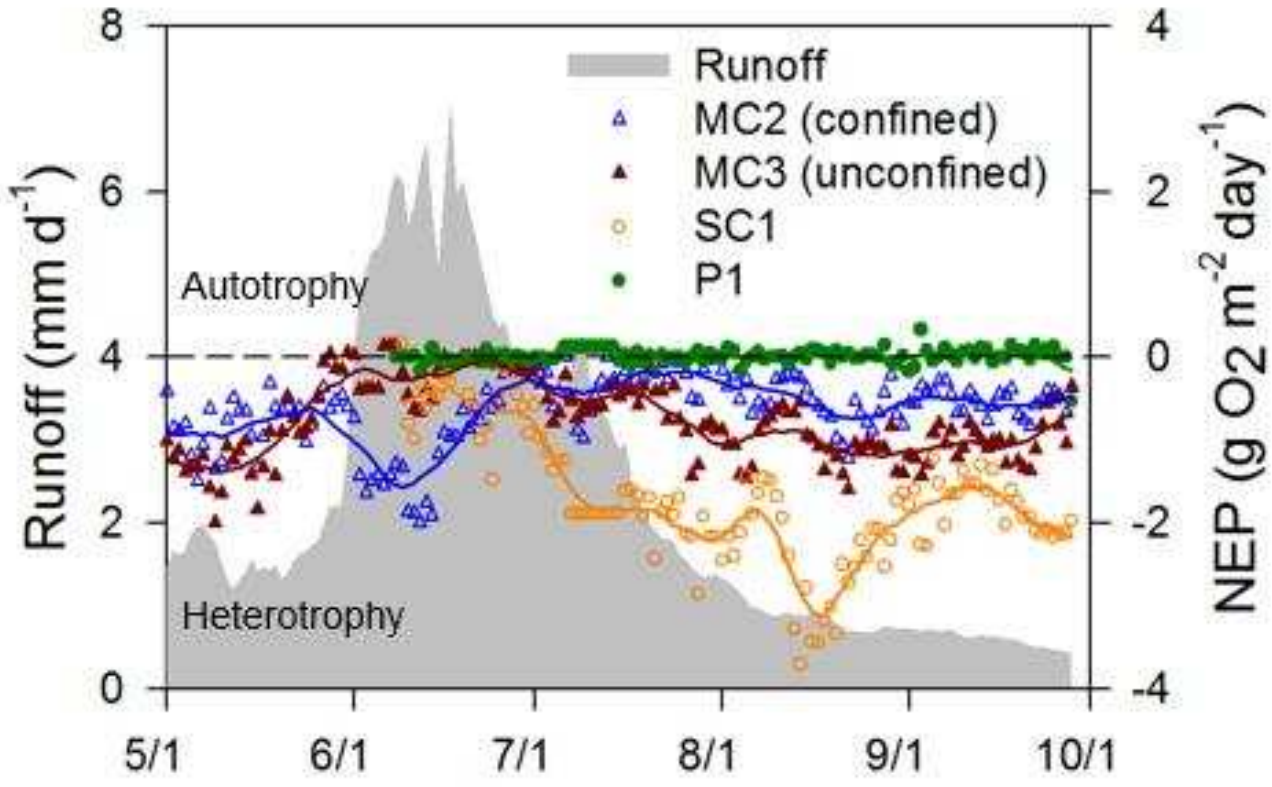

Figure 11. Main channel (MC2) runoff with net ecosystem production (NEP) at main channel sites MC2 (confined outflow) and MC3 (unconfined outflow), and a floodplain side-channel, SC1, and pond, P1. Metabolism metrics were calculated using an open system, single station dissolved oxygen approach. Main channel monitoring began on May 1st and floodplain water-body monitoring began on June 9th. All sites were net heterotrophic except P1, which was slightly net autotrophic.

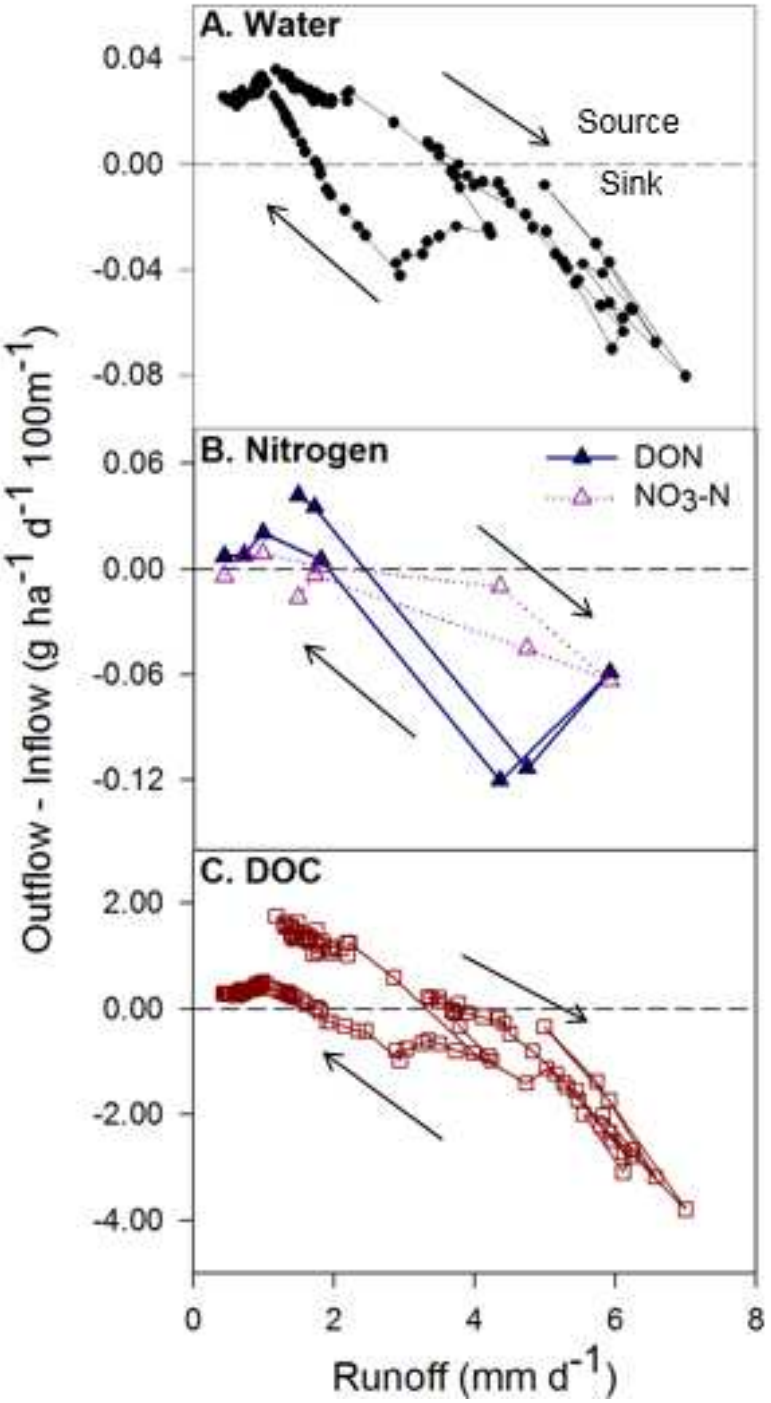

Figure 12. Source-sink dynamics for a) water, b) dissolved organic nitrogen (DON) and nitrogen as nitrate (NO_3-N), and c) dissolved organic carbon (DOC) fluxes along the unconfined segment as a function of runoff. The unconfined segment was a sink for N at all flows above 2 mm d^{-1} and a sink for water and DOC when flows exceeded ~4 mm d^{-1} on the rising limb and down to ~2 mm d^{-1} on the falling limb of the hydrograph. This indicates that the floodplain had greater sink behavior on the falling- relative to the rising-limb of the hydrograph for a given flow state.

7. TABLES

Table 1. Physical characteristics for the confined and unconfined segments of North Saint Vrain Creek in Wild Basin Watershed, Rocky Mountain National Park, Colorado.

	Confined Segment	**Unconfined Segment**
Drainage area (km^2)	82	88
Average reach elevation (m)	2560	2050
Main channel length (m)	400	2100
Morphology	Confined valley Single-thread Moderate gradient Pool-riffle channel	Unconfined valley bottom Multi-thread Low-gradient Pool-riffle main channel

Table 2. Summary (mean ± SD) of temperature and runoff data at main channel sites MC1, MC2, and MC3, and a floodplain side-channel, SC1, and pond, P1. The confined segment is bracketed by MC1 and MC2, and the unconfined segment is bracketed by MC2 and MC3. Data are from May - October 2015.

	MC1	**MC2**	**MC3**	**SC1**	**P1**
Temperature (°C)	7.4 ± 3.4	7.7 ± 3.4	8.4 ± 3.6	9.8 ± 5.9	10.4 ± 3.7
Runoff (mm day^{-1})	2.14 ± 1.45	2.23 ± 1.79	2.38 ± 1.28	---	---

Table 3. Hydrometric characteristics of side-channels and ponds in the unconfined segment floodplain that were intermittently- or never- surface water connected with the main channel from May – October 2015. For surface connected sites, high connectivity referred to the period of time in which the sites were hydrologically inundated by overbank flooding from the main channel. For sites with no surface water connectivity with the main channel, shifts in the strength of connectivity likely reflected transitions in subsurface flow-paths.

	Site	Onset of high connectivity[1]	End of high connectivity[1]	Date when Dry[2]	Water surface elevation (m) (mean ± SD)
Intermittent surface water connectivity	SC1	5/30	7/12	---	2540.06 ± 0.11
	SC2	5/30	7/12	---	2543.48 ± 0.13
	SC3	5/30	7/12	---	2538.60 ± 0.07
	SC4	5/30	7/12	---	2537.41 ± 0.22
	SC5	5/26	7/14	9/12	2541.84 ± 0.15
No surface water connectivity	SC6	---	---	8/05	2538.90 ± 0.12
	P1	6/01	7/09	---	2541.26 ± 0.03
	P2	5/30	6/26	8/13	2539.04 ± 0.25
	P3	5/31	7/10	---	2538.89 ± 0.24
	P4	5/30	7/08	---	2542.86 ± 0.09
	P5	---	---	---	2538.51 ± 0.06
	P6	5/31	7/12	7/12	2543.77 ± 0.11

[1]blanks indicate no observed change in the strength of connectivity during the monitoring period
[2]blanks indicate that the site contained water at the end of the monitoring period

Table 4. Summary (mean ± SD) of dissolved nutrient concentrations (mg L^{-1}) at main channel sites MC1, MC2 and MC3, and a floodplain side-channel, SC1, and pond, P1. The confined segment is bracketed by MC1 and MC2, and the unconfined segment is bracketed by MC2 and MC3. Nutrient concentrations are listed for nitrogen as ammonium (NH_4-N), nitrogen as nitrate (NO_3-N), dissolved organic nitrogen (DON), and dissolved organic carbon (DOC). Data are from grab samples taking approximately every other week from May – October 2015.

	MC1	**MC2**	**MC3**	**SC1**	**P1**
NH_4-N	0.02 ± 0.01	0.02 ± 0.01	0.02 ± 0.08	0.03 ± 0.02	0.06 ± 0.08
NO_3-N	0.07 ± 0.04	0.08 ± 0.04	0.07 ± 0.04	0.05 ± 0.05	0.03 ± 0.01
DON	0.09 ± 0.04	0.10 ± 0.07	0.10 ± 0.05	0.20 ± 0.18	0.12 ± 0.05
DOC	3.50 ± 2.05	2.95 ± 1.87	3.56 ± 1.81	4.74 ± 1.71	3.24 ± 1.81

Table 5. Summary (mean ± SD) of daily fluxes normalized for watershed area (g ha^{-1} d^{-1}) of nitrogen as nitrate (NO_3-N), dissolved organic nitrogen (DON), and dissolved organic carbon (DOC) from main channel sites MC1, MC2, and MC3. The confined segment is bracketed by MC1 and MC2, and the unconfined segment is bracketed by MC2 and MC3. DOC fluxes are from 15-minute time series, and nitrogen fluxes are from grab samples taken approximately every other week from May - October 2015.

	MC1	**MC2**	**MC3**
NO_3-N	1.79 ± 1.94	2.49 ± 2.88	2.27 ± 2.47
DON	1.75 ± 2.00	2.63 ± 2.74	2.55 ± 1.85
DOC	79.8 ± 73.5	84.9 ± 94.3	85.9 ± 80.8

Table 6. Summary (mean ± SD) of ecosystem metabolism metrics gross primary productivity (GPP), ecosystem respiration (ER), and net ecosystem productivity (NEP) (g O_2 m^{-2} d^{-1}) at main channel sites MC2 (confined outflow) and MC3 (unconfined outflow), and a floodplain side-channel, SC1, and pond, P1. Main channel data extends from May 1st – September 28th, and floodplain data extends from June 9th – September 28th 2015.

	MC2	**MC3**	**SC1**	**P1**
GPP	+0.09 ± 0.14	+1.01 ± 0.76	+0.93 ± 0.50	+0.57 ± 0.33
ER	-0.72 ± 0.50	-1.77 ± 1.10	-2.64 ± 1.00	-0.56 ± 0.32
NEP	-0.63 ± 0.44	-0.76 ± 0.48	-1.70 ± 0.80	+0.01 ± 0.09

8. REFERENCES

Aerts, R. 1997. Climate, leaf litter chemistry and leaf litter decomposition in terrestrial ecosystems: a triangular relationship. Oikos:439-449.

Allan, J. D., and M. M. Castillo. 2007. Stream ecology: structure and function of running waters. Springer Science & Business Media.

Arscott, D. B., K. Tockner, and J. Ward. 2001. Thermal heterogeneity along a braided floodplain river (Tagliamento River, northeastern Italy). Canadian Journal of Fisheries and Aquatic Sciences **58**:2359-2373.

Battin, T. J., L. A. Kaplan, S. Findlay, C. S. Hopkinson, E. Marti, A. I. Packman, J. D. Newbold, and F. Sabater. 2008. Biophysical controls on organic carbon fluxes in fluvial networks. Nature Geosci **1**:95-100.

Bayley, P. B. 1995. Understanding large river: floodplain ecosystems. BioScience **45**:153-158.

Bellmore, J., and C. Baxter. 2014. Effects of geomorphic process domains on river ecosystems: A comparison of floodplain and confined valley segments. River research and applications **30**:617-630.

Bernot, M. J., D. J. Sobota, R. O. Hall, P. J. Mulholland, W. K. Dodds, J. R. Webster, J. L. Tank, L. R. Ashkenas, L. W. Cooper, C. N. Dahm, S. V. Gregory, N. B. Grimm, S. K. Hamilton, S. L. Johnson, W. H. McDowell, J. L. Meyer, B. Peterson, G. C. Poole, H. M. Valett, C. Arango, J. J. Beaulieu, A. J. Burgin, C. Crenshaw, A. M. Helton, L. Johnson, J. Merriam, B. R. Niederlehner, J. M. O'Brien, J. D. Potter, R. W. Sheibley, S. M. Thomas, and K. Y. M. Wilson. 2010. Inter-regional comparison of land-use effects on stream metabolism. Freshwater Biology **55**:1874-1890.

Bott, T. 1996. Primary productivity and community respiration. Pages 553-556 *in* F. R. Haur, Lamberti, G.A., editor. Methods in Stream Ecology. Academic Press, San Diego, CA.

Boyd, C. E., and D. Teichert-Coddington. 1992. Relationship between wind speed and reaeration in small aquaculture ponds. Aquacultural engineering **11**:121-131.

Braddock, W., and J. Cole. 1990. Geologic map of Rocky Mountain National Park and vicinity. Pages Map I-1973, scale 1971:1950,1000, 1971 sheet. U.S. Geological Survey Miscellaneous Investigation Series, Colorado.

Briggs, M. A., L. K. Lautz, J. M. McKenzie, R. P. Gordon, and D. K. Hare. 2012. Using high-resolution distributed temperature sensing to quantify spatial and temporal variability in vertical hyporheic flux. Water Resources Research **48**:W02527.

Burchsted, D., M. Daniels, R. Thorson, and J. Vokoun. 2010. The River Discontinuum: Applying Beaver Modifications to Baseline Conditions for Restoration of Forested Headwaters. BioScience **60**:908-922.

Cabezas, A., M. Gonzalez-Sanchís, B. Gallardo, and F. A. Comín. 2011. Using continuous surface water level and temperature data to characterize hydrological connectivity in riparian wetlands. Environmental monitoring and assessment **183**:485-500.

Chapra, S., and D. Di Toro. 1991. Delta Method For Estimating Primary Production, Respiration, And Reaeration In Streams. Journal of Environmental Engineering **117**:640-655.

Cirmo, C. P., and C. T. Driscoll. 1996. The impacts of a watershed CaCO3 treatment on stream and wetland biogeochemistry in the Adirondack Mountains. Biogeochemistry **32**:265-297.

Cirmo, C. P., and J. J. McDonnell. 1997. Linking the hydrologic and biogeochemical controls of nitrogen transport in near-stream zones of temperate-forested catchments: a review. Journal of Hydrology **199**:88-120.

Correll, D. L., T. E. Jordan, and D. E. Weller. 2000. Beaver pond biogeochemical effects in the Maryland Coastal Plain. Biogeochemistry **49**:217-239.

Devito, K., P. Dillon, and B. Lazerte. 1989. Phosphorus and nitrogen retention in five Precambrian shield wetlands. Biogeochemistry **8**:185-204.

Dingman, S. 2002. Physical Hydrology. 2 edition. Prentice Hall, Upper Saddle River, New Jersey.

Dominguez, F., E. Rivera, D. Lettenmaier, and C. Castro. 2012. Changes in winter precipitation extremes for the western United States under a warmer climate as simulated by regional climate models. Geophysical Research Letters **39**.

Elmore, H., and W. West. 1961. Effect of water temperature on stream reaeration. Journal of Sanitary Engineering Division ASCE:59-71.

Fellows, C. S., M. H. Valett, and C. N. Dahm. 2001. Whole‐stream metabolism in two montane streams: Contribution of the hyporheic zone. Limnology and Oceanography **46**:523-531.

Fisher, S. G., L. J. Gray, N. B. Grimm, and D. E. Busch. 1982. Temporal succession in a desert stream ecosystem following flash flooding. Ecological monographs **52**:93-110.

González-Pinzón, R., M. Peipoch, R. Haggerty, E. Martí, and J. H. Fleckenstein. 2016. Nighttime and daytime respiration in a headwater stream. Ecohydrology **9**:93-100.

Hey, D. L., J. A. Kostel, W. G. Crumpton, W. J. Mitsch, and B. Scott. 2012. The roles and benefits of wetlands in managing reactive nitrogen. Journal of Soil and Water Conservation **67**:47A-53A.

Hill, A. R., C. F. Labadia, and K. Sanmugadas. 1998. Hyporheic zone hydrology and nitrogen dynamics in relation to the streambed topography of a N-rich stream. Biogeochemistry **42**:285-310.

Hill, W. R., M. G. Ryon, and E. M. Schilling. 1995. Light limitation in a stream ecosystem: responses by primary producers and consumers. Ecology:1297-1309.

Hupp, C. R., A. R. Pierce, and G. B. Noe. 2009. Floodplain geomorphic processes and environmental impacts of human alteration along coastal plain rivers, USA. Wetlands **29**:413-429.

Jones, J. B., S. G. Fisher, and N. B. Grimm. 1995. Vertical Hydrologic Exchange and Ecosystem Metabolism in a Sonoran Desert Stream. Ecology **76**:942-952.

Junk, W. J., P. B. Bayley, and R. E. Sparks. 1989. The flood pulse concept in river-floodplain systems. Canadian special publication of fisheries and aquatic sciences **106**:110-127.

Kilpatrick, F. A., and E. D. Cobb. 1985. Measurement of discharge using tracers. Department of the Interior, US Geological Survey.

Lamberti, G. A., S. V. Gregory, L. R. Ashkenas, R. C. Wildman, and A. G. Steinman. 1989. Influence of channel geomorphology on retention of dissolved and particulate matter in a Cascade Mountain stream.

Lamberti, G. A., and A. D. Steinman. 1997. A comparison of primary production in stream ecosystems. Journal of the North American Benthological Society **16**:95-104.

Lazar, J. G., K. Addy, A. J. Gold, P. M. Groffman, R. A. McKinney, and D. Q. Kellogg. 2015. Beaver Ponds: Resurgent Nitrogen Sinks for Rural Watersheds in the Northeastern United States. Journal of environmental quality **44**:1684-1693.

Malard, F., A. Mangin, U. Uehlinger, and J. Ward. 2001. Thermal heterogeneity in the hyporheic zone of a glacial floodplain. Canadian Journal of Fisheries and Aquatic Sciences **58**:1319-1335.

Malard, F., K. Tockner, and J. V. Ward. 2000. Physico-chemical heterogeneity in a glacial riverscape. Landscape Ecology **15**:679-695.

McClain, M. E., E. W. Boyer, C. L. Dent, S. E. Gergel, N. B. Grimm, P. M. Groffman, S. C. Hart, J. W. Harvey, C. A. Johnston, and E. Mayorga. 2003. Biogeochemical hot spots and hot moments at the interface of terrestrial and aquatic ecosystems. Ecosystems **6**:301-312.

McKnight, D. M., K. E. Bencala, G. W. Zellweger, G. R. Aiken, G. L. Feder, and K. A. Thorn. 1992. Sorption of dissolved organic carbon by hydrous aluminum and iron oxides occurring at the confluence of Deer Creek with the Snake River, Summit County, Colorado. Environmental Science & Technology **26**:1388-1396.

Mertes, L. A. 1997. Documentation and significance of the perirheic zone on inundated floodplains. Water Resources Research **33**:1749-1762.

Mitsch, W. J., C. L. Dorage, and J. R. Wiemhoff. 1979. Ecosystem dynamics and a phosphorus budget of an alluvial cypress swamp in southern Illinois. Ecology:1116-1124.

Montgomery, D. R., and J. M. Buffington. 1997. Channel-reach morphology in mountain drainage basins. Geological Society of America Bulletin **109**:596-611.

Mulholland, P., C. S. Fellows, J. Tank, N. Grimm, J. Webster, S. Hamilton, E. Martí, L. Ashkenas, W. Bowden, and W. Dodds. 2001. Inter‐biome comparison of factors controlling stream metabolism. Freshwater Biology **46**:1503-1517.

Odum, H. T. 1956. Primary production in flowing waters. Limnology and Oceanography **1**:102-117.

Owens, M. 1974. Measurements on non-isolated natural communities in running waters. Pages 111-119 *in* R. A. Vollenweider, editor. A Manual on Methods for Measuring Primary Production in Aquatic Environments. Blackwell Scientific Publications Oxford, UK.

Peterson, B. J., J. E. Hobbie, A. E. Hershey, M. A. Lock, T. E. Ford, J. R. Vestal, V. L. McKinley, M. A. Hullar, M. C. Miller, and R. M. Ventullo. 1985. Transformation of a tundra river from heterotrophy to autotrophy by addition of phosphorus. Science **229**:1383-1386.

Pierson, D., T. Fegel, C. Rhoades, and B. Starr. 2016. Summary of Analysis Methods for the Rocky Moutnain Research Station Biogeochemistry Laboratory.*in* R. M. R. Center, U. S. F. Service, and U. S. D. o. Agriculture, editors.

Pinay, G., N. E. Haycock, C. Ruffinoni, and R. M. Holmes, editors. 1994. The role of denitrification in nitrogen removal in river corridors. Mitsch, W.j>.

Powers, S. M., R. A. Johnson, and E. H. Stanley. 2012. Nutrient retention and the problem of hydrologic disconnection in streams and wetlands. Ecosystems **15**:435-449.

Reckendorfer, W., C. Baranyi, A. Funk, and F. Schiemer. 2006. Floodplain restoration by reinforcing hydrological connectivity: expected effects on aquatic mollusc communities. Journal of Applied ecology **43**:474-484.

Roberts, B. J., and P. J. Mulholland. 2007. In‐stream biotic control on nutrient biogeochemistry in a forested stream, West Fork of Walker Branch. Journal of Geophysical Research: Biogeosciences (2005–2012) **112**.

Sibold, J. S., T. T. Veblen, and M. E. González. 2006. Spatial and temporal variation in historic fire regimes in subalpine forests across the Colorado Front Range in Rocky Mountain National Park, Colorado, USA. Journal of Biogeography **33**:631-647.

Sinsabaugh, R., M. Osgood, and S. Findlay. 1994. Enzymatic models for estimating decomposition rates of particulate detritus. Journal of the North American Benthological Society:160-169.

Stanford, J. A., and J. Ward. 1993. An ecosystem perspective of alluvial rivers: connectivity and the hyporheic corridor. Journal of the North American Benthological Society:48-60.

Tank, J. L., E. J. Rosi-Marshall, N. A. Griffiths, S. A. Entrekin, and M. L. Stephen. 2010. A review of allochthonous organic matter dynamics and metabolism in streams. Journal of the North American Benthological Society **29**:118-146.

Tockner, K., F. Malard, and J. Ward. 2000. An extension of the flood pulse concept. Hydrological processes **14**:2861-2883.

Tockner, K., D. Pennetzdorfer, N. Reiner, F. Schiemer, and J. Ward. 1999. Hydrological connectivity, and the exchange of organic matter and nutrients in a dynamic river–floodplain system (Danube, Austria). Freshwater Biology **41**:521-535.

Uehlinger, U. 2000. Resistance and resilience of ecosystem metabolism in a flood‐prone river system. Freshwater Biology **45**:319-332.

Uehlinger, U. 2006. Annual cycle and inter‐annual variability of gross primary production and ecosystem respiration in a floodprone river during a 15‐year period. Freshwater Biology **51**:938-950.

Uehlinger, U., and M. W. Naegeli. 1998. Ecosystem metabolism, disturbance, and stability in a prealpine gravel bed river. Journal of the North American Benthological Society:165-178.

Vitousek, P. M., J. D. Aber, R. W. Howarth, G. E. Likens, P. A. Matson, D. W. Schindler, W. H. Schlesinger, and D. G. Tilman. 1997. Human alteration of the global nitrogen cycle: sources and consequences. Ecological applications **7**:737-750.

Vollenweider, R. A. 1974. A manual on methods for measuring primary production in aquatic environments. I.B.P. Handbook 12, Blackwell, Oxford, UK.

Ward, J. V., and J. Stanford. 1995. Ecological connectivity in alluvial river ecosystems and its disruption by flow regulation. Regulated Rivers: Research & Management **11**:105-119.

Westbrook, C. J., D. J. Cooper, and B. W. Baker. 2006. Beaver dams and overbank floods influence groundwater-surface water interactions of a Rocky Mountain riparian area. Water Resources Research **42**.

Whittecar, G. R., and W. L. Daniels. 1999. Use of hydrogeomorphic concepts to design created wetlands in southeastern Virginia. Geomorphology **31**:355-371.

Wiegner, T. N., L. A. Kaplan, J. D. Newbold, and P. H. Ostrom. 2005. Contribution of dissolved organic C to stream metabolism: a mesocosm study using 13C-enriched tree-tissue leachate. Journal of the North American Benthological Society **24**:48-67.

Wohl, E. 2001. Virtual rivers: lessons from mountain rivers of the Colorado Front Range. Yale University Press, New Haven, CT.

Young, R. G., C. D. Matthaei, and C. R. Townsend. 2008. Organic matter breakdown and ecosystem metabolism: functional indicators for assessing river ecosystem health. Journal of the North American Benthological Society **27**:605-625.

9. APPENDIX A

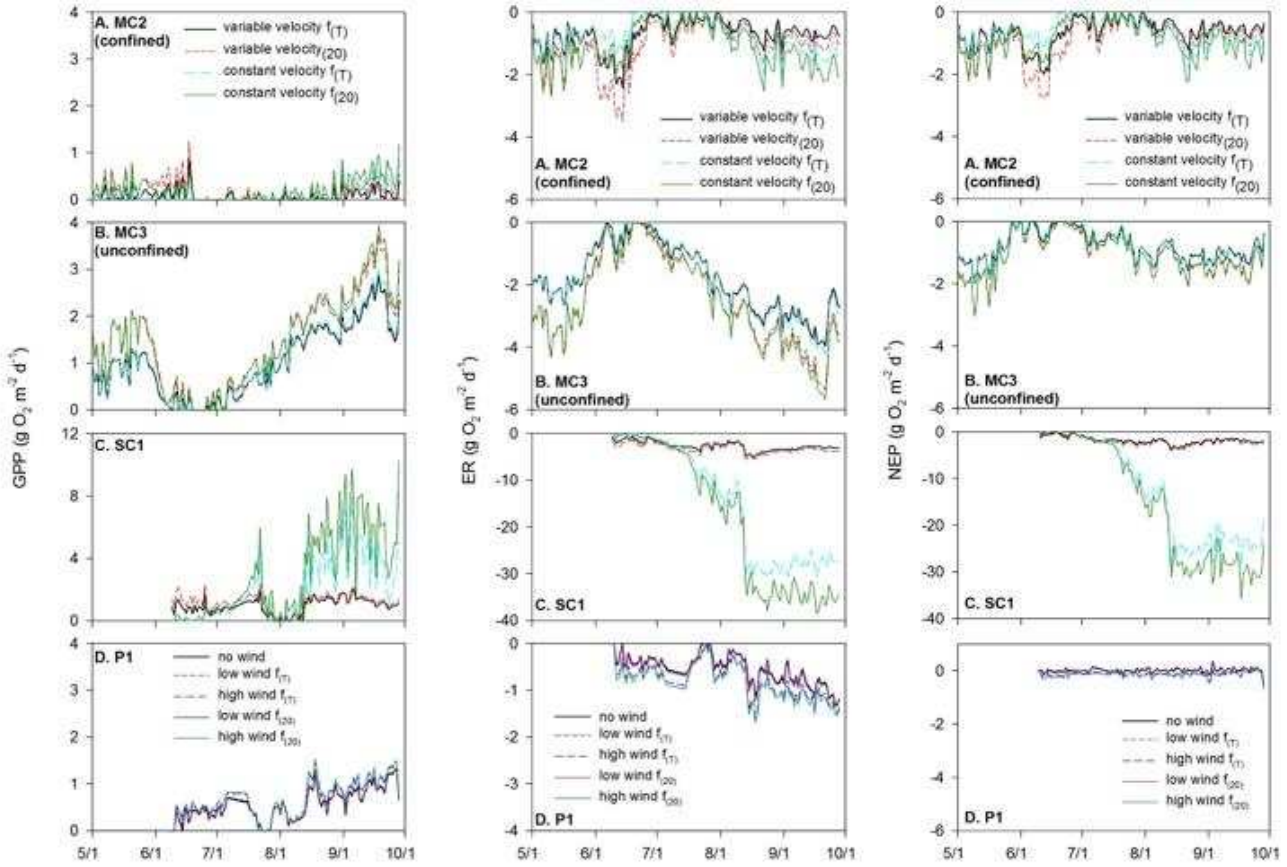

Supplemental Figure 1. Gross primary productivity (GPP), ecosystem respiration (ER), and net ecosystem production (NEP) calculated for a) MC2, the confined segment outflow, b) MC3, the unconfined segment outflow, c) a floodplain side-channel (SC1), and d) a floodplain pond (P1) under different scenarios for calculating reaeration. While there were little differences between

reaeration coefficients calculated at standard temperature and those adjusted for daily temperatures, incorporating daily changes in velocity sometimes made substantial differences in metabolism, particularly at SC1.

Supplemental Table 1. Different scenarios used to calculate the reaeration coefficient for MC2 (confined outflow), MC3 (unconfined outflow), the side-channel (SC1) and the pond (P1). *V* is water velocity (cm s), *H* is average water height (cm), *t* is mean daily temperature (°C) and *X* is wind speed (m s^{-1}).

Site	Reaeration Equation	Scenario
MC2, MC3, and SC1	$50.8 * V_{daily}^{0.67} * H^{-0.85}$	1. mean daily water velocity and mass transfer coefficient at standard temperature
	$\left(50.8 * V_{daily}^{0.67} * H^{-0.85}\right) * 1.024^{t-20}$	2. mean daily water velocity and mass transfer coefficient corrected for temperature
	$50.8 * V_{constant}^{0.67} * H^{-0.85}$	3. constant (total mean) water velocity and mass transfer coefficient at standard temperature
	$(50.8 * V_{constant}^{0.67} * H^{-0.85}) * 1.024^{t-20}$	4. constant (total mean) water velocity and mass transfer coefficient corrected for water temperature
P1	----	1. no wind
	0.017*X* - 0.014, *X* = 0.8	2. low wind and reaeration at standard temperature
	0.017*X* - 0.014 * 1.024^{t-20}, *X* = 0.8	3. low wind and reaeration corrected for temperature
	0.017*X* - 0.014, *X* = 4.5	4. high wind and reaeration at standard temperature
	0.017*X* - 0.014 * 1.024^{t-20}, *X* = 4.5	5. high wind and reaeration corrected for temperature